

321  
/ DISTRIBUTION OF FLUORESCENTLY LABELED ACTIN

IN LIVING CELLS,

by

STEPHEN DOUGLAS GLACY

B.S., Kansas State University, 1979

A MASTER'S THESIS

submitted in partial fulfillment of the

requirements for the degree

MASTER OF SCIENCE


Division of Biology

KANSAS STATE UNIVERSITY

Manhattan, Kansas

1982

Approved:

  
Major Professor

LD  
2668  
IT4  
1982  
G52  
C.2

A11202 609770

# TABLE OF CONTENTS

	<u>Page</u>
I. ACKNOWLEDGEMENTS . . . . .	1
II. CHAPTER 1. SUBCELLULAR DISTRIBUTION OF RHODAMINE- ACTIN MICROINJECTED INTO LIVING FIBROBLASTIC CELLS. .	2
A. Introduction . . . . .	3
B. Materials and Methods . . . . .	9
1. Cell culture procedures . . . . .	9
2. Fluorescent labeling of actin . . . . .	9
3. Viscosity measurements . . . . .	10
4. Microinjection and microscopy . . . . .	10
C. Results . . . . .	12
1. Controls . . . . .	12
a. Viscosities of actin solutions . . . . .	12
b. Non-specific binding of rhodamine-actin . . . . .	12
c. Microinjection of FITC-ovalbumin. . . . .	12
d. SDS-PAGE of rhodamine-actin . . . . .	13
2. Time-course of rhodamine-actin incorporation. .	13
3. Rhodamine-actin incorporation and focal contacts	23
D. Discussion . . . . .	28
E. References . . . . .	32
III. CHAPTER 2. PATTERN AND TIME-COURSE OF RHODAMINE- ACTIN INCORPORATION IN CARDIAC MYOCYTES . . . . .	38
A. Introduction . . . . .	39
B. Materials and Methods . . . . .	45
1. Cell culture procedures . . . . .	45
2. Fluorescent labeling of actin . . . . .	45
3. Microinjection and microscopy . . . . .	45

	<u>Page</u>
C. Results . . . . .	47
D. Discussion . . . . .	51
E. References . . . . .	53
IV. APPENDICES . . . . .	55
A. The microinjection system . . . . .	56
B. Labeling of actin with iodoacetamido tetramethyl rhodamine . . . . .	65
C. Cell culture procedures . . . . .	68
D. F12 nutrient medium . . . . .	69
E. Salt solutions and buffers . . . . .	70
F. Trypsin solutions . . . . .	71
G. Skeletal muscle acetone powder . . . . .	72
H. Skeletal actin isolation from acetone powder . . . . .	73
I. Bio-Rad protein assay . . . . .	74
J. Viscometry assay of actin . . . . .	75
K. Incubation of fixed, permeabilized cells with rhodamine-actin. . . . .	76

# LIST OF FIGURES

	<u>Page</u>
Figure 1. F-Actin distribution in non-muscle cells . . . . .	6
Figure 2. Polymerization of actin. . . . .	8
Figure 3. Capillary viscometry of labeled and unlabeled F-actin solutions. . . . .	15
Figure 4. Incubation of permeabilized, fixed cells with rhodamine-actin . . . . .	17
Figure 5. Microinjection of FITC-ovalbumin . . . . .	19
Figure 6. SDS-PAGE of rhodamine-actin . . . . .	21
Figure 7. Time-course of rhodamine-actin incorporation in fibroblastic cells . . . . .	25
Figure 8. Fluorescence distribution and focal contacts . . . . .	27
Figure 9. General structure of the sarcomere . . . . .	42
Figure 10. Representation of sliding filaments on a molecular level . . . . .	44
Figure 11. Time-course of rhodamine-actin incorporation into cardiac myocytes . . . . .	50
Figure A. Micropipette formation . . . . .	60
Figure B. Side-view of micropipette chamber . . . . .	62
Figure C. Microinjection chamber . . . . .	64
Figure D. Labeling procedure . . . . .	67



Acknowledgements

This research was supported by NIH grant HD-07193 to Gary W. Conrad.

## CHAPTER 1

# SUBCELLULAR DISTRIBUTION OF RHODAMINE-ACTIN MICROINJECTED INTO LIVING FIBROBLASTIC CELLS

## Introduction

In non-muscle cells, actin may comprise as much as 15% of total cellular protein (1), and has been implicated in such dynamic cellular activities as cytokinesis (2), membrane ruffling (3,4) and cell spreading in vitro (5). The evidence for actin involvement in these functions stems mainly from the observations that in areas of high motile activity, such as the cleavage furrow in dividing cells or the leading edge in actively moving cells, actin is present in a form and distribution that may readily lend itself to force generation (see ref. 3 and Fig.1).

A combination of techniques, including biochemical studies (6), electron microscopy (3,4,7) and fluorescence microscopy (5,7), has demonstrated that actin exists in cultured non-muscle cells in both the polymerized and non-polymerized forms. Non-polymerized actin, which may account for 35-50% of the total actin in non-muscle cells (6), is probably not present as soluble G-actin, but more likely is complexed with one or more of the numerous actin-binding proteins of non-muscle cells (8). Since the general ionic conditions of the cytoplasm are such that 98% of the actin should be in the filamentous form (9), it is obvious that non-muscle cells possess regulatory systems that maintain large portions of their actin in a non-polymerized state, possibly for employment in dynamic cellular processes by controlled rapid polymerization (Fig. 2).

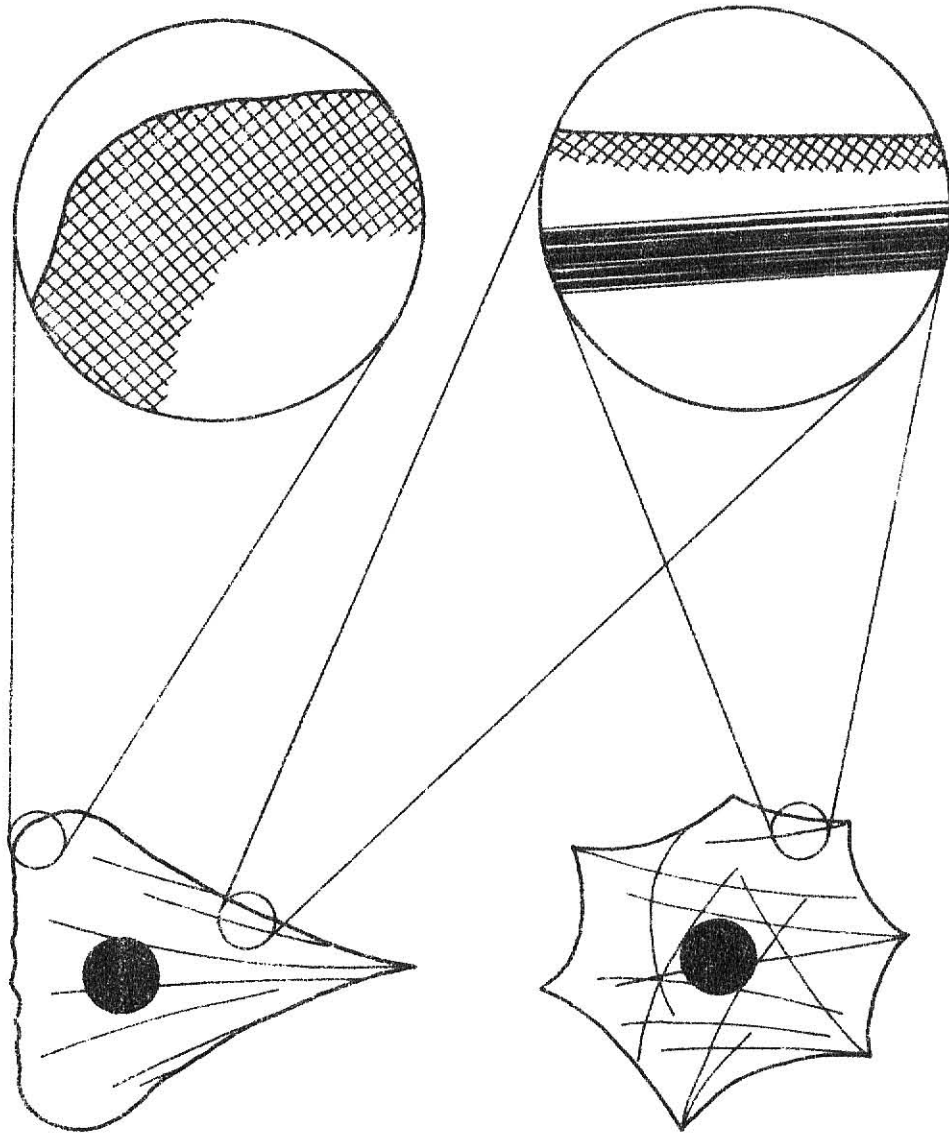
Recently, Wang and Taylor introduced a technique involving micro-injection of fluorochrome-labeled contractile proteins into cells and subsequent determination of their fate (10,11). Other investigators have extended this approach to the study of cellular contractile functions by introducing a variety of proteins and substances into cells: actin (12-18), tropomyosin (19), calmodulin (20), tubulin (21), 130K protein (22),

alpha-actinin (23-25), anti-actin antibodies (26), anti-intermediate filament antibodies (27,28), anti-myosin antibodies (29,30), aequorin (31), phalloidin (32-36), calcium (37), chlorotetracycline (38) and N-ethylmaleimide-modified heavy meromyosin (39).

In the present study I have examined some dynamic properties of rhodamine-labeled actin microinjected into cultured chick fibroblastic cells. My results indicate that exogenous rhodamine-actin is rapidly incorporated into subcellular structures and areas containing F-actin and playing a role in cell motility, i.e., stress fibers and ruffling membranes. Within minutes after introduction of rhodamine-actin into cells, a rapid and selective increase in fluorescence was observed in ruffling membranes, stress fibers and cellular areas corresponding to focal contacts.



Figure 1. Representation of filamentous actin distribution in tissue culture cells of various morphologies. With light microscopy, actin-containing stress fibers can be seen. In wedge-shaped cells, stress fibers usually are oriented the length of the cell, whereas in polygonal cells they are typically more random. With electron microscopy, the microfilament network can be seen. This network is in a cortical region and is particularly prominent in the leading edge.



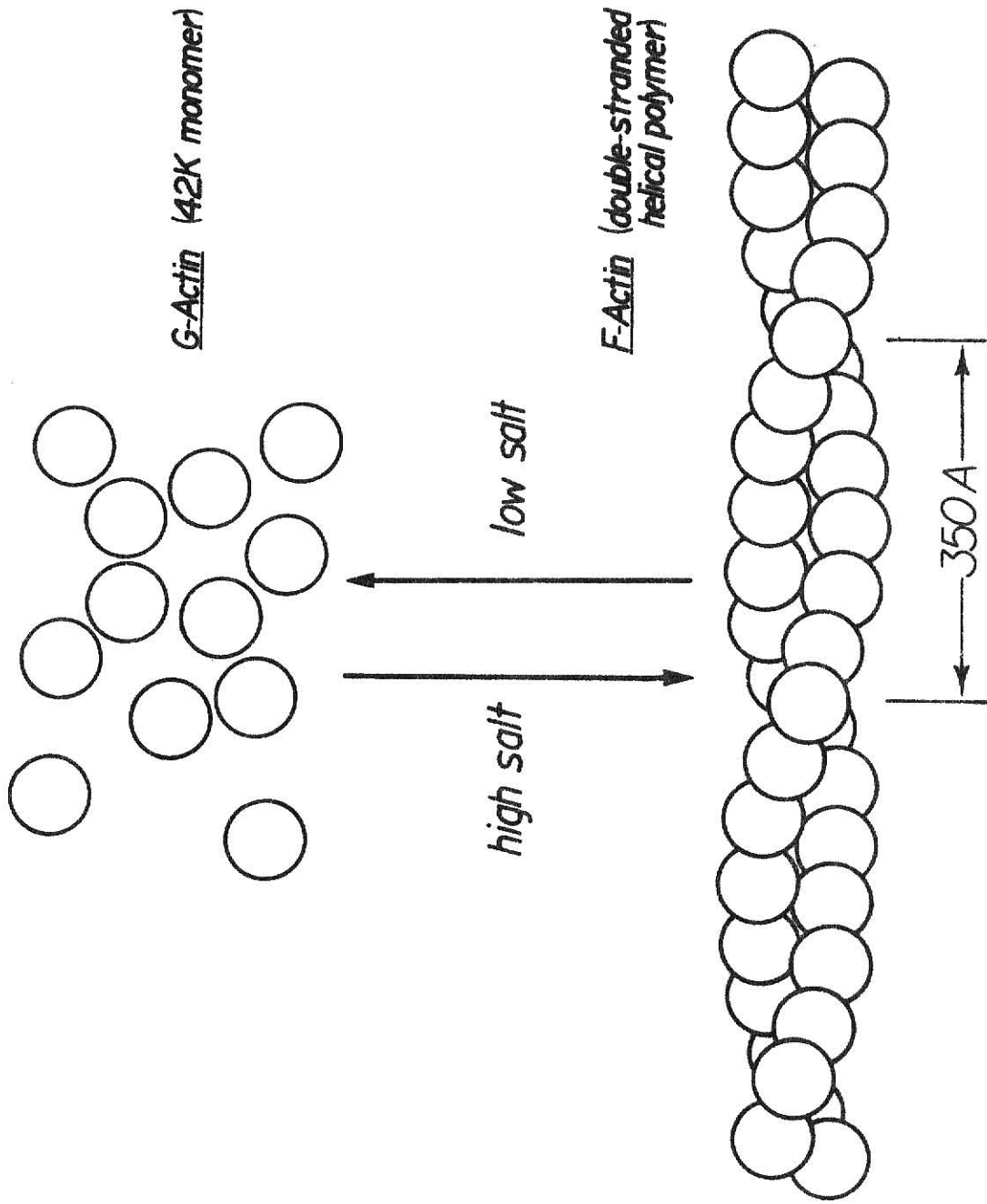
By electron microscopy

By light microscopy





Figure 2. Polymerization of actin to a double-stranded helical polymer occurs in the presence of high salt concentrations. Dialyzing F-actin against low salt concentration buffers will revert it to G-actin.



## Materials and Methods

### Cell Culture Procedures

Heart ventricles from 12-14 d chick embryos were minced in sterile calcium- and magnesium-free Saline G (CMF Sal G), and enzymatically dissociated into single cells with 0.2% trypsin in CMF Sal G for 30 min at 37° C. Digestions were terminated by addition of an equal volume of F-12 nutrient medium containing 10% fetal calf serum, 30 µg/ml penicillin G and 50 µg/ml streptomycin sulfate. Cell suspensions were filtered through single layers of Nitex cloth, collected by centrifugation, resuspended in fresh nutrient medium and plated into 60 mm diameter Falcon tissue culture dishes. The dishes were kept in a humid atmosphere of 5% CO<sub>2</sub>/95% air at 37° C. Prior to microinjection, primary cultures were trypsinized and replated at lower densities onto glass coverslips and cultured for an additional 24-48 h.

### Fluorescent Labeling of Actin

Skeletal muscle actin was prepared from an acetone powder of chicken breast muscle (40) and dialyzed against Buffer G (2 mM Tris-HCl, 0.4 mM ascorbate, 0.2 mM ATP, 0.1 mM CaCl<sub>2</sub>, pH 8.0) to obtain G-actin. Concentrations of unlabeled G-actin were determined spectrophotometrically by absorption at 290 nm using an extinction coefficient of 0.63 ml mg<sup>-1</sup> cm<sup>-1</sup> (42). Concentrations of rhodamine-actin were measured by the Bradford protein assay (41), which was standardized against a spectrophotometrically determined G-actin solution. Ten mg of iodoacetamido tetramethyl rhodamine (Research Organics, Cleveland, Ohio) was placed into 0.5 ml of acetone, vortexed, and added to 3 ml of Buffer G containing 8 mM ATP at pH 10.5-11. This dye solution was added dropwise to 12-15 mg of G-actin in 4 ml

of Buffer G. Mixtures were titrated to pH 8.5 with 0.1N NaOH and stirred for 2 h at room temperature. The actin was polymerized by addition of 3 M KCl and 1 M  $MgCl_2$  to final concentrations of 100 mM and 2 mM, respectively, and sedimented by centrifugation at 100,000 g for 3 h. F-actin pellets were depolymerized in 600 mM KI, desalted on a Sephadex G-25 column (42) and clarified by centrifugation at 100,000 g for 2 h. The rhodamine-actin was taken through another polymerization/depolymerization cycle and stored at 4° C for no more than 24 h before use in experiments.

### Viscosity Measurements

Viscosities of labeled and unlabeled F-actin solutions were measured using a Cannon-Manning semi-microviscometer Model 150 (46).

### Microinjection and Microscopy

The microinjection system used was similar to that described by Diacumakos (43). Coverslips with attached cells were inverted to form the top of a microinjection chamber, which consisted of a U-shaped plastic support resting upon a 45x50 mm No. 2 coverglass. During microinjection and observations within 5 min post-injection, chambers were filled with Saline G. For observations during later periods of the experiments, Saline G was replaced with nutrient medium. Injection micropipettes were made from 1.2x100 mm Omega Dot capillary tubes (F. Haer, Brunswick, ME) which had been soaked consecutively in acetone and nitric acid, and rinsed extensively with 3X glass-distilled water and dried. The micropipettes were pulled on a DKI 700C capillary puller (David Kopf Instruments, Tujunga, CA) and shaped on a laboratory-made microforge. Micropipettes were backloaded with rhodamine-actin at 2-3 mg/ml in Buffer G, and mounted onto a micromanipulator (E. Leitz, Rockleigh, NJ). Injections,

observations and photography were performed on a Zeiss Standard microscope equipped with epifluorescence optics. Interference reflection microscopy was done as previously described (44). Exposures were taken on Ilford XP-1 35 mm film and developed for 6.5 min at 40° C in Ilford XP-1 chemicals.

The amount of rhodamine-actin microinjected into cells was estimated by the following means. Cells were injected in a perinuclear region with the micropipette remaining in the cell until about 20-30% of the cell area, as microscopically viewed, displayed the injection fluid. By approximating cell area to cell volume, and knowing the concentrations of rhodamine-actin (2-3 mg/ml) and endogenous actin in fibroblasts (8 mg/ml) (45), the injected rhodamine-actin was estimated to represent roughly 11% of total endogenous actin ( $30\% \times 3 \text{ mg/ml} / 100\% \times 8 \text{ mg/ml} = 0.11$ ).

## Results

### Controls

Viscosity of Actin Solutions: The ability of actin to polymerize with a concomitant increase in viscosity is a fundamental biochemical property of the protein. Ostwald capillary viscometry was used to compare the viscometric properties of unlabeled actin and rhodamine-actin. Figure 3 summarizes these studies and indicates that in the protein concentration range tested, both unlabeled and labeled preparations displayed similar viscosities.

Non-Specific Binding of Rhodamine-Actin: In a recent report (46), rhodamine-labeled  $\alpha$ -actinin was shown to bind to stress fibers in demembranated fibroblasts in an arrangement similar to that of immunofluorescence with anti- $\alpha$ -actinin antibodies and to microinjected  $\alpha$ -actinin. To ensure that the patterns I obtained in microinjected cells did not reflect passive binding of rhodamine-actin, cardiac myocytes and fibroblasts were permeabilized with 0.5% Triton X-100 and 0.37% formaldehyde in PBS for 5 min, and post-fixed in 3.7% formaldehyde in PBS for 20 min, before incubation with rhodamine-actin (200  $\mu$ g/ml) in Buffer G for 10 min. Figure 4 shows that this treatment resulted in low uniform fluorescence in the cytoplasm, comparatively higher nuclear fluorescence and no discernable binding of the probe to either stress fibers or myofibrils.

Microinjection of FITC-Ovalbumin: As a second control to demonstrate that patterns of fluorescence in microinjected cells represented functional incorporation of rhodamine-actin, living fibroblastic cells were injected with FITC-ovalbumin, a non-cytoskeletal protein. Only uniform fluorescence was seen throughout cells treated in this manner (Fig.5 ).

SDS-PAGE of Rhodamine-Actin: To critically interpret fluorescence patterns observed in microinjected cells it was important to ascertain the level of fluorescent substances that were not associated with polymerization-competent rhodamine-actin. At least four sources of non-specific fluorescence were possible: (a) free dye: any rhodamine that had not reacted covalently with actin, yet was carried through the purification procedures; (b) degradation products of rhodamine-actin: spontaneous or proteolytic degradation of rhodamine-actin, resulting in non-functional fluorescent peptides; (c) trace protein contaminants: such as tropomyosin, which may have contaminated actin preparations and were labeled with the fluorescent dye; and (d) denatured rhodamine-actin: actin that has denatured during the labeling and purification procedure. The purity of rhodamine-actin was monitored by gel electrophoresis. Figure 6 shows rhodamine-actin subjected to electrophoresis in a 10% SDS-polyacrylamide gel. Other than very slight fluorescence associated with the dye front, only the actin band shows fluorescence. Electrophoresis in SDS-polyacrylamide gels cannot reveal whether actin migrating at 42K is native or denatured. To ensure the biochemical integrity of the probe, the rhodamine-actin was subjected to at least two polymerization/depolymerization cycles after labeling with iodoacetamido tetramethyl rhodamine, and always used within 24 h for microinjection.

#### Time-Course of Rhodamine-Actin Incorporation

Results reported in this paper are based on observations of at least 300 microinjected fibroblastic cells. Immediately following microinjection, rhodamine-actin spread rapidly through the cytoplasm of fibroblastic cells and resulted in uniform cellular fluorescence. Less than 5 min after injection there was a pronounced fluorescence increase in cell





Figure 3. Ostwald capillary viscometry of labeled (○) and unlabeled (●) F-actin solutions. G-actin solutions were polymerized by the addition of 3 M KCl and 1 M  $\text{MgCl}_2$  to final concentrations of 100 mM and 2 mM, respectively, then incubated for 6 hours at 25<sup>0</sup> C. The solid line indicates the slope generated by the unlabeled F-actin preparation.

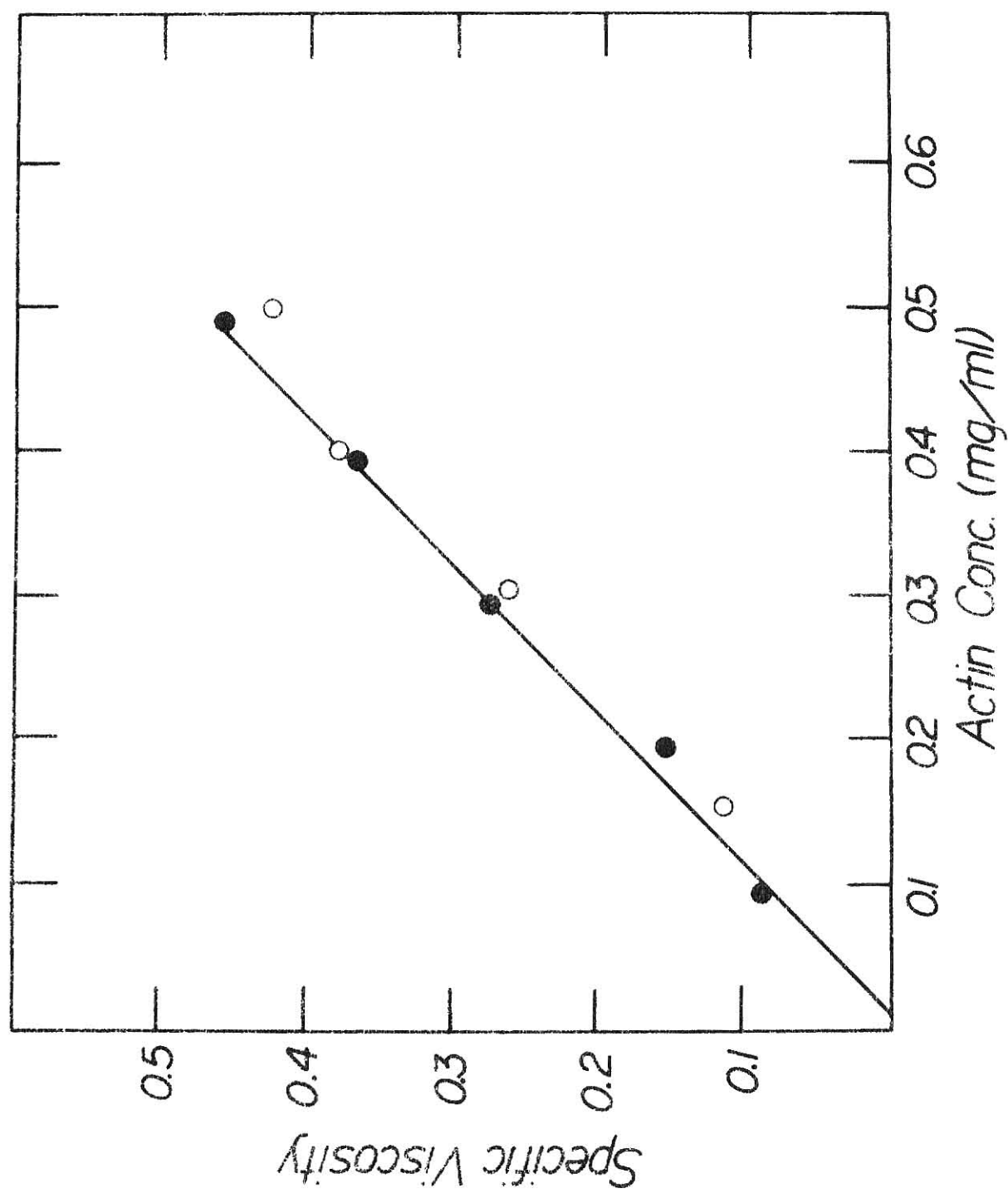




Figure 4. Phase contrast and matching fluorescence images of permeabilized, fixed cells incubated with rhodamine-actin. The phase contrast micrograph (a) demonstrates the numerous myofibrils of the myocytes (single arrows), and stress fibers of the fibroblastic cells (double arrows). The matching fluorescence photomicrograph (b) shows that neither the myofibrils nor the stress fibers bind the rhodamine-actin.

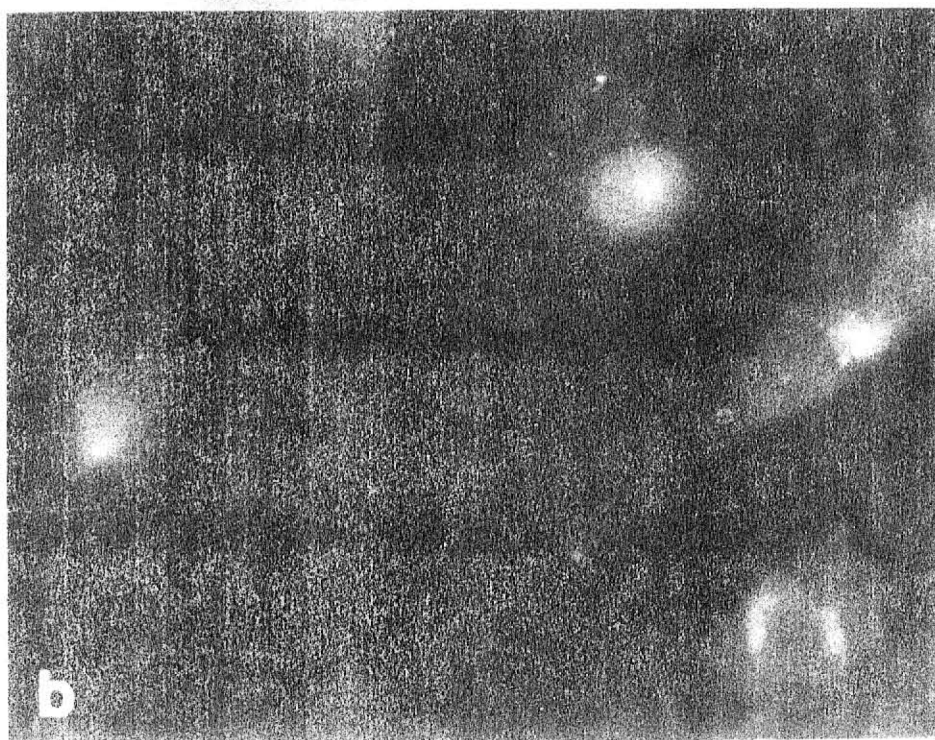
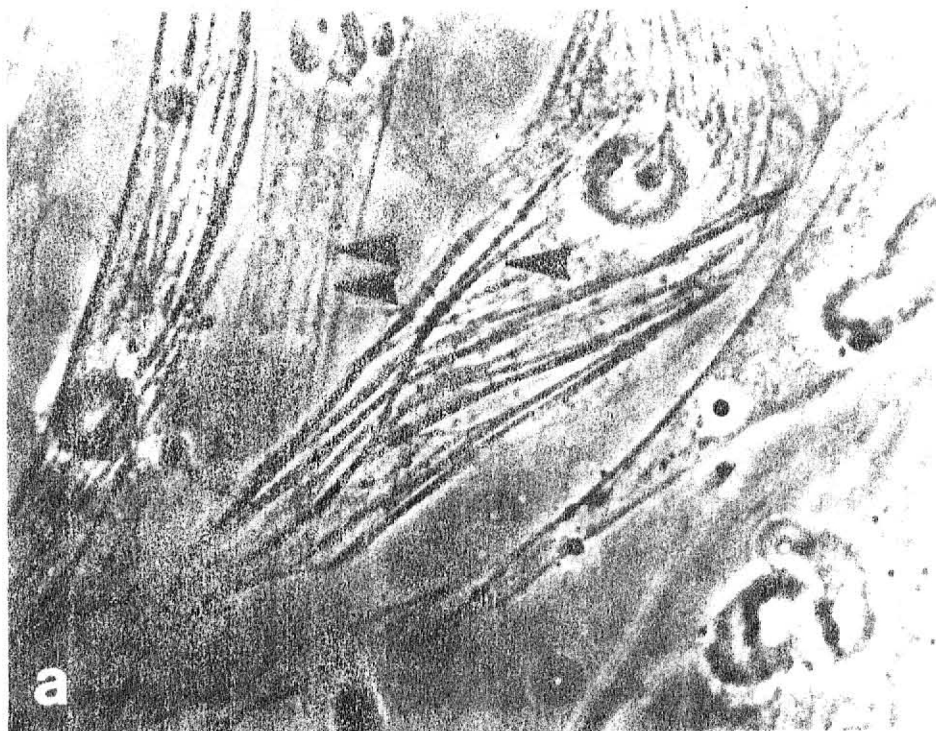




Figure 5. Fluorescence micrograph of a cell which had been micro-injected with FITC-ovalbumin. The fluorescence distribution is uniform through the cytoplasm and appears to correspond in intensity to cell thickness.

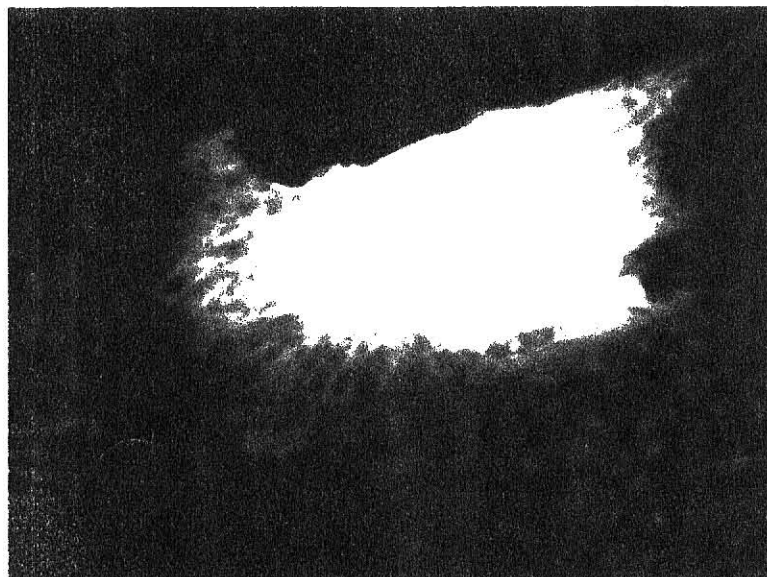
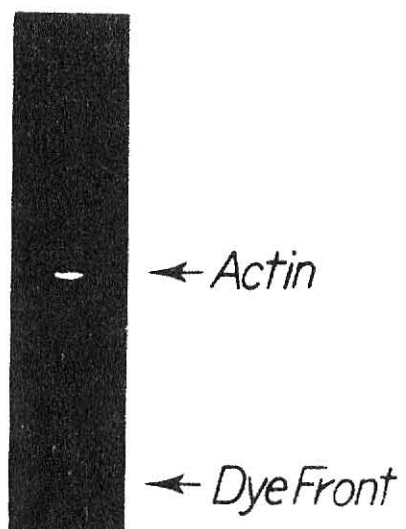






Figure 6. Fluorescence photograph of rhodamine-actin electrophoresed in SDS-polyacrylamide. Other than small amounts of fluorescence at the dye front and the fluorescence associated with the actin band, the lane shows no other fluorescence.



areas corresponding to ruffling membranes, with maximum fluorescence levels obtained in these regions about 5 min post-injection (Fig. 7b). In some cells, the difference in fluorescence intensity between the ruffling membrane and more interior areas of the cell was quite substantial (Fig. 7b). Some of the interior cellular regions, particularly those directly adjacent to the ruffling membrane, were as non-fluorescent as the surrounding substrate. Peripheral fluorescence in areas of the ruffling membrane was of uniform width (single arrowhead, Fig. 7b) or quite varying in width (double arrowhead, Fig. 7b).

Fluorescence in stress fibers initially appeared about 5 min post-injection (Fig. 7b), and by 10 min was quite prominent (Fig. 7d). The fluorescence level of stress fibers continued to increase until about 20 min post-injection, then tended to remain constant. Additionally, incorporation of rhodamine-actin into stress fibers was uniform along the length of the fibers, with no polarity or periodicities of distribution observed. In some cells, polygonal fiber networks (47) also incorporated rhodamine-actin with rates similar to stress fibers (data not shown).

In general, a correlation existed between cellular morphology and distribution of rhodamine-actin. Polygonal-shaped cells with many stress fibers usually incorporated most of the injected rhodamine-actin into stress fibers, leaving very little interfibrillary cytoplasmic fluorescence. Wedge-shaped cells frequently displayed a uniform fluorescence upon microinjection with rhodamine-actin, with fewer fluorescent stress fibers than cells with polygonal morphologies. However, these generalities did not hold for all cells observed. Figures 7e and f show a wedge-shaped cell at 1 h post-injection. Most of the rhodamine-actin had been incorporated into the many stress fibers oriented with the long axis of the

cell. Note especially the very low levels of fluorescence in the interfibrillary space of the perinuclear region, and the lack of fluorescence in the putative leading edge.

#### Rhodamine-Actin Incorporation and Focal Contacts

In approximately 50% of microinjected cells, particularly bright patches of fluorescence were noticed at about 5-10 min post-injection. These patches were similar to fluorescent patterns seen in cells stained with anti-vinculin antibodies (44). By interference reflection microscopy, many of these fluorescent patches corresponded to focal contacts (Fig. 8). In cells observed after 20-30 minutes post-injection, the fluorescent patches decreased in prominence as stress fibers that led to such focal contacts progressively incorporated increasing amounts of rhodamine-actin.



Figure 7. Phase contrast and corresponding fluorescent images of chick heart fibroblastic cells microinjected with rhodamine-actin. Time points following injection are 5 min (a and b), 10 min (c and d), and 1 hour (e and f). At 5 min post-injection, a distinct band of fluorescence is evident along the cell periphery in the region of the ruffling membrane (b), which may be of uniform width (single arrowheads) or of varying width (double arrowheads). By 10 min after injection, fluorescence can be seen in both the ruffling membrane and stress fibers. Figures e and f show a wedge-shaped cell at 1 hour post-injection, demonstrating incorporation of most rhodamine-actin into stress fibers.

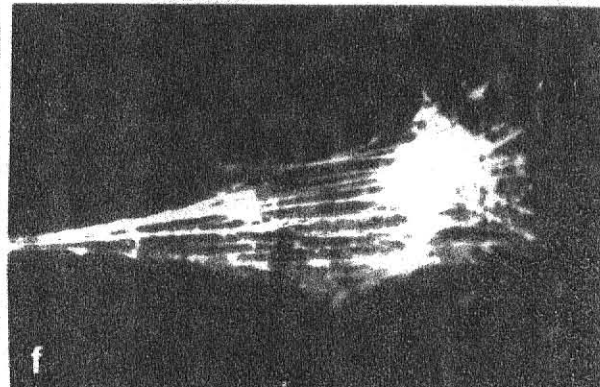
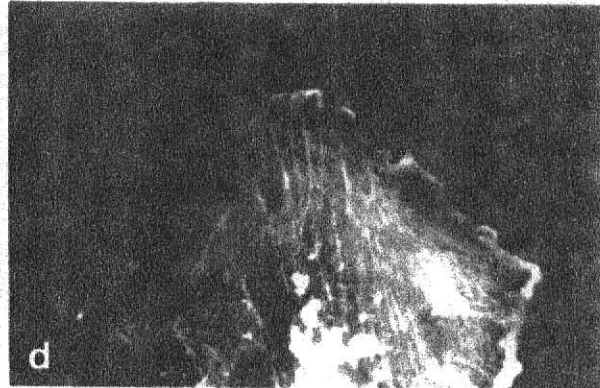
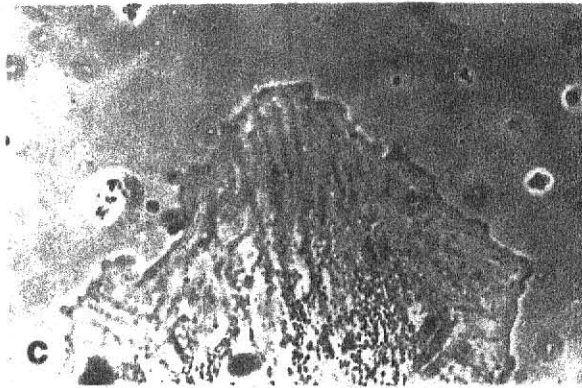
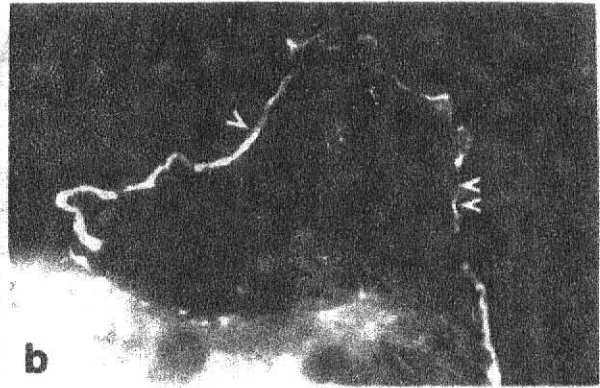
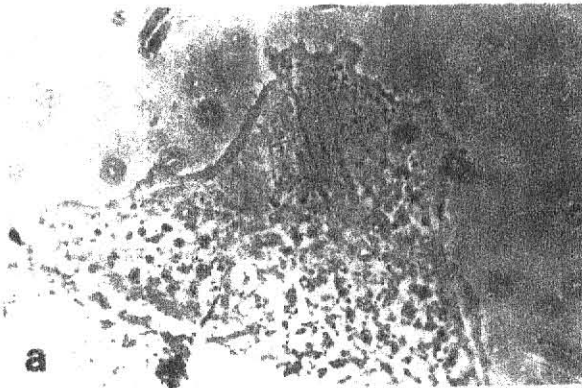
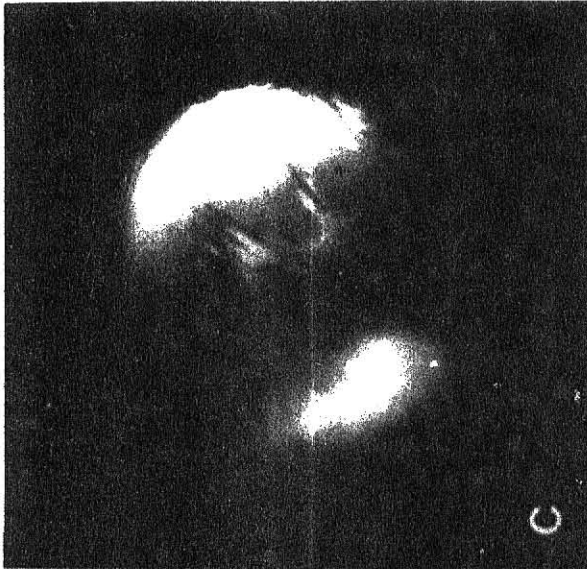






Figure 8. Phase contrast, fluorescence and interference reflection images of a portion of a chick heart fibroblastic cell microinjected with rhodamine-actin at 10 min post-injection. By fluorescence microscopy (b) bright patches of fluorescence can be seen at and near the cell perimeter which correspond to phase-dense regions seen by phase contrast microscopy (a) and to focal contacts seen by interference reflection microscopy (c).



### Discussion

This paper presents information demonstrating that fibroblastic cells rapidly incorporate rhodamine-actin into selective subcellular structures which have been implicated in cell motility and cytoskeletal functions. Leading edges and ruffling membranes are areas commonly present in tissue culture cells undergoing locomotion, and in this study, showed a marked increase in fluorescence following microinjection, reaching a maximum level by 5 min post-injection. Stress fibers usually are assigned a cytoskeletal role because of the inverse relationship between their number in a cell and the rate of cellular movement (5). In the present study, stress fibers began to show fluorescence approximately 5 min post-injection and, in contrast to ruffling membranes, continued to increase in fluorescent intensity until a maximum level was achieved about 20 min post-injection.

Results described in this manuscript corroborate and extend findings recently reported by Kreis et al. (18). In their study of rhodamine-actin dynamics in chicken gizzard cells by fluorescence photobleaching recovery, they discovered that the leading edge displayed the highest rate of rhodamine-actin mobility of all cellular domains studied. Additionally, their reported half-time for fluorescence recovery in stress fibers of 10 min agrees well with my observation that maximum levels of fluorescence were achieved in stress fibers by 20 min post-injection.

At least two possibilities exist to explain the relatively faster incorporation of actin into ruffling membranes. Microfilaments of the ruffling membrane are usually present as a network of individual filaments, rather than as the bundles characterizing stress fibers (4). Thus, the filaments of this region are probably more accessible to microinjected actin. The faster rate of fluorescence increase, therefore, may reflect

simply higher availability of polymerization sites in filaments of the ruffling membrane than in those of stress fibers. Conversely, faster incorporation rates in the ruffling membrane may stem from the high motile activity characterizing the area. Breakdown, assembly and rearrangement of actin filaments probably are required for these motile activities, which include extension and retraction of the lamellapodium. Faster rates of incorporation, therefore, may reflect increased filament turnover, which is presumed to require a readily available pool of G-actin.

Morphologically, stress fibers are relatively unchanging structures. It is possible to observe single stress fibers in some cells by phase contrast optics for several hours without noting drastic changes in length or appearance (3). Thus, the swift appearance of fluorescence in stress fibers of microinjected cells is surprising and suggests that these morphologically stable structures are in fact relatively dynamic at a molecular level. Moreover, the incorporation of fluorescence uniformly along the length of stress fibers suggests that they contain numerous polymerization sites, and hence may be comprised of many short microfilaments. Focal contacts are discrete areas where the underside of the cell is within 15 nm of the substrate. These areas usually correspond to adhesion plaques and are generally located at the terminating tips of microfilament bundles (48). The results presented here demonstrate that there is a preferential recruitment of rhodamine-actin into focal contacts of microinjected fibroblastic cells. It is not clear whether this selective incorporation is of functional significance, or merely reflects the high number of potential polymerization sites in the area.

Metabolic half-lives of actin and myosin in cultured fibroblasts have been reported to be a minimum of 2.5 d (49). Therefore, the rapid appearance of rhodamine-actin in F-actin-containing structures of microinjected cells

probably does not represent metabolic protein turnover (i.e., biosynthesis and degradation). More likely, results of the present study suggest a constant cycling of actin through these structures, with little protein degradation. Additionally, the width of ruffling membrane fluorescence, as well as stress fiber length, displayed no discernible increase during incorporation of rhodamine-actin. It seems likely then that as rhodamine-actin molecules were being incorporated, other actin molecules were being removed. Initially, this exchange would be predominately unlabeled actin molecules removed in exchange for rhodamine-actin molecules incorporated. During later periods, both labeled and unlabeled actin molecules would participate in assembly and disassembly. This might explain the rapid initial appearance of fluorescence and its subsequent persistence. Filamentous actin in vitro undergoes a continuous exchange with available G-actin, without a net change of overall filament length (45). My findings suggest a similar phenomenon for actin filaments in vivo.

The results of the present study support the increasingly widespread notion of the dynamic nature of actin in vertebrate cells. A considerable portion of the actin in non-muscle cells exists in the non-polymerized state (6), despite cytosolic ionic conditions which, if present uniformly throughout the cell, prescribe that most of the actin should be in a filamentous form. The numerous actin binding proteins may serve to maintain this large pool of non-polymerized actin (8). It therefore seems likely that a balance of factors affects the state of actin polymerization in the cytosol: ionic conditions favoring polymerization versus actin binding proteins maintaining filament length and favoring non-polymerized forms. With these cellular conditions in mind one must then consider the possible perturbing effects of increasing the cell's intracellular pool of actin. The introduction of pure G-actin into the

cytoplasm is bound to upset, to an unknown degree, the equilibrium between polymerized and non-polymerized actin. The tendency will be for the injected actin to polymerize immediately. However, at the injection concentrations used in this study (2-3 mg/ml), cells appeared to possess the ability to control the polymerization of the exogenous actin. The initial uniform fluorescence upon injection, followed by subsequent incorporation, suggests a sufficient abundance of actin-binding proteins to prevent immediate polymerization. It is interesting to note, however, that cells do appear to have definite limits to their ability to control injected actin. Microinjection of rhodamine-actin at concentrations 3 times higher than those used in the present study resulted in the almost immediate formation of long wavy filaments or structures resembling actin paracrystals (data not shown). These unusual actin structures were observed in cells up to two hours post-injection, but no long-term study has been done to see if cells eventually depolymerized them.

Various microinjection studies recently have indicated the dynamic nature of the cytoplasm. The results of the present study indicate that biochemically functional rhodamine-actin can be introduced into living cells, without affecting viability. This method continues to be of value in the study of cell motility and other dynamic activities.

### References

1. Bray, D., and C. Thomas. 1975. The actin content of fibroblasts. *Biochem. J.* 147:221-228.
2. Schroeder, T. E. 1973. Actin in dividing cells: Contractile ring filaments bind heavy meromyosin. *Proc. Natl. Acad. Sci. U.S.A.* 70:1688-1692.
3. Buckley, I. K. 1981. Fine-structural and related aspects of non-muscle-cell motility. *Cell and Muscle Motility* 1:135-203.
4. Small, J. V., G. Isenberg, and J. E. Celis. 1978. Polarity of actin at the leading edge of cultured cells. *Nature.* 272:638-639.
5. Herman, I. M., N.J. Crisona, and T. D. Pollard. 1981. Relation between cell activity and the distribution of cytoplasmic actin and myosin. *J. Cell Biol.* 90:84-91.
6. Blikstad, I., and L. Carlsson. 1982. On the dynamics of the microfilament system in HeLa cells. *J. Cell Biol.* 93:122-128.
7. Willingham, M. C., S. S. Yamada, P. J. A. Davies, A. V. Rutherford, M. G. Gallo, and I. Pastan. 1981. Intracellular localization of actin in cultured fibroblasts by electron microscopic immunocytochemistry. *J. Histochem. Cytochem.* 29:17-37.
8. Weeds, A. 1982. Actin-binding proteins: regulators of cell architecture and motility. *Nature.* 296:811-816.
9. Korn, E. D. 1978. Biochemistry of actomyosin-dependent cell motility. *Proc. Natl. Acad. Sci. U.S.A.* 75:588-599.
10. Taylor, D. L., and Y.-L. Wang. 1978. Molecular cytochemistry: Incorporation of fluorescently labeled actin into living cells. *Proc. Natl. Acad. Sci. U.S.A.* 75:857-861.



11. Taylor, D. L., and Y.-L. Wang. 1980. Fluorescently labelled molecules as probes of the structure and function of living cells. *Nature*. 284:405-410.
12. Sanger, J. W., J. M. Sanger, T. E. Kreis, and B. M. Jockusch. 1980. Reversible translocation of cytoplasmic actin into the nucleus caused by dimethyl sulfoxide. *Proc. Natl. Acad. Sci. U.S.A.* 77: 5268-5272.
13. Birchmeier, C., T. E. Kreis, H. M. Eppenberger, K. H. Winterhalter, and W. Birchmeier. 1980. Corrugated attachment membrane in WI-38 fibroblasts: Alternating fibronectin fibers and actin-containing focal contacts. *Proc. Natl. Acad. Sci. U.S.A.* 77:4108-4112.
14. Kreis, T. E., K. H. Winterhalter, and W. Birchmeier. 1979. In vivo distribution and turnover of fluorescently labeled actin microinjected into human fibroblasts. *Proc. Natl. Acad. Sci. U.S.A.* 76:3814-3818.
15. Taylor, D. L., Y.-L. Wang, and J. M. Heiple. 1980. Contractile basis of ameboid movement. VII. The distribution of fluorescently labeled actin in living amebas. *J. Cell Biol.* 86:590-598.
16. Gawlitta, W., W. Stockem, J. Wehland, and K. Weber. 1980. Organization and spatial arrangement of fluorescein-labeled native actin microinjected into normal locomoting and experimentally influenced Amoeba proteus. *Cell Tissue Res.* 206:181-191.
17. Wang, Y.-L., and D. L. Taylor. 1979. Distribution of fluorescently labeled actin in living sea urchin eggs during early development. *J. Cell Biol.* 82:672-679.
18. Kreis, T. E., B. Geiger, and J. Schlessinger. 1982. Mobility of microinjected rhodamine actin within living chicken gizzard cells determined by fluorescence photobleaching recovery. *Cell*. 29:835-845.

19. Wehland, J., and K. Weber. 1980. Distribution of fluorescently labeled actin and tropomyosin after microinjection in living tissue culture cells as observed with TV image intensification. *Exp. Cell Res.* 127:397-408.
20. Hamaguchi, Y., and F. Iwasa. 1980. Localization of fluorescently labeled calmodulin in living sea urchin eggs during early development. *Biomed. Res.* 1:502-509.
21. Keith, C. H., J. R. Feramisco, and M. Shelanski. 1981. Direct visualization of fluorescein-labeled microtubules in vitro and in microinjected fibroblasts. *J. Cell Biol.* 88:234-240.
22. Burridge, K., and J. R. Feramisco. 1980. Microinjection and localization of a 130K protein in living fibroblasts: a relationship to actin and fibronectin. *Cell.* 19:587-595.
23. Feramisco, J. R., and S. H. Blose. 1980. Distribution of fluorescently labeled  $\alpha$ -actinin in living and fixed fibroblasts. *J. Cell Biol.* 86:608-615.
24. Feramisco, J. R. 1979. Microinjection of fluorescently labeled  $\alpha$ -actinin into living fibroblasts. *Proc. Natl. Acad. Sci. U.S.A.* 76:3967-3971.
25. Kreis, T. E., and W. Birchmeier. 1980. Stress fiber sarcomeres of fibroblasts are contractile. *Cell.* 22:555-561.
26. Rungger, D., E. Rungger-Brändle, C. Chaponnier, and G. Gabbiani. 1979. Intracellular injection of anti-actin antibodies into Xenopus oocytes blocks chromosome condensation. *Nature* 282:320-321.
27. Klymkowsky, M. W. 1981. Intermediate filaments in 3T3 cells collapse after intracellular injection of a monoclonal anti-intermediate filament antibody. *Nature.* 291:249-251.

28. Lin, J. J.-C., and J. R. Feramisco. 1981. Disruption of the *in vivo* distribution of the intermediate filaments in fibroblasts through the microinjection of a specific monoclonal antibody. *Cell*. 24:185-193.
29. Mabuchi, I., and M. Okuno. 1977. The effect of myosin antibody on the division of starfish blastomeres. *J. Cell Biol.* 74:251-263.
30. Kiehart, D. P., I. Mabuchi, and S. Inoué. 1982. Evidence that myosin does not contribute to force production in chromosome movement. *J. Cell Biol.* 94:165-178.
31. Taylor, D. L., J. R. Blinks, and G. Reynolds. 1980. Contractile basis of ameboid movement. VIII. Aequorin luminescence during ameboid movement, endocytosis, and capping. *J. Cell Biol.* 86: 599-607.
32. Wehland, J., M. Osborn, and K. Weber. 1980. Phalloidin associates with microfilaments after microinjection into tissue culture cells. *Eur. J. Cell Biol.* 21:188-194.
33. Wehland, J., and K. Weber. 1981. Actin rearrangement in living cells revealed by microinjection of a fluorescent phalloidin derivative. *Eur. J. Cell Biol.* 24:176-183.
34. Stockem, W., K. Weber, and J. Wehland. 1978. The influence of microinjected phalloidin on locomotion, protoplasmic streaming and cytoplasmic organization in *Amoeba proteus* and *Physarum polycephalum*. *Cytobiologie* 18:114-131.
35. Götz von Olenhusen, K., and K. E. Wohlfarth-Bottermann. 1979. Evidence for actin transformation during the contraction-relaxation cycle of cytoplasmic actomyosin: cycle blockade by phalloidin injection. *Cell Tissue Res.* 196:455-470

36. Wehland, J., M. Osborn, and K. Weber. 1977. Phalloidin-induced actin polymerization in the cytoplasm of cultured cells interferes with cell locomotion and growth. *Proc. Natl. Acad. Sci. U.S.A.* 74: 5613-5617.
37. Kiehart, D. P. 1981. Studies on the in vivo sensitivity of spindle microtubules to calcium ions and evidence for a vesicular calcium-sequestering system. *J. Cell Biol.* 88:604-617.
38. Gawlitta, W., W. Stockem, J. Wehland, and K. Weber. 1980. Pinocytosis and locomotion of amoebae. XV. Visualization of  $Ca^{++}$ -dynamics by chlorotetracycline (CTC) fluorescence during induced pinocytosis in living Amoeba proteus. *Cell Tissue Res.* 213:9-20.
39. Meeusen, R. L., J. Bennett, and W. Z. Cande. 1980. Effect of microinjected N-ethylmaleimide-modified heavy meromyosin on cell division in amphibian eggs. *J. Cell Biol.* 86:858-865.
40. Spudich, J. A., and S. Watt. 1971. The regulation of rabbit skeletal muscle contraction. *J. Biol. Chem.* 246:4866-4871.
41. Bradford, M. M. 1976. A rapid and sensitive method for the quantitation of microgram quantities of protein utilizing the principle of protein-dye binding. *Anal. Biochem.* 72:248-254.
42. Wang, Y.-L., and D. L. Taylor. 1980. Preparation and characterization of a new molecular cytochemical probe: 5-iodoacetamidofluorescein-labeled actin. *J. Histochem. Cytochem.* 28:1198-1206.
43. Diacumakos, E. G. 1973. Methods for micromanipulation of human somatic cells in culture. *Meth. Cell Biol.* 7:287-311.
44. Geiger, B. 1979. A 130K protein from chicken gizzard: its localization at the termini of microfilament bundles in cultured chicken cells. *Cell.* 18:193-205.

45. Pollard, T. D. 1981. Cytoplasmic contractile proteins. *J. Cell Biol.* 91:156s-165s.
46. Geiger, B. 1981. The association of rhodamine-labelled  $\alpha$ -actinin with actin bundles in demembranated cells. *Cell Biol. Intl. Reports* 5:627-634.
47. Gordon, W. E., III, and A. Bushnell. 1979. Immunofluorescent and ultrastructural studies of polygonal microfilament networks in respreading non-muscle cells. *Exp. Cell Res.* 120:335-348.
48. Abercrombie, M., and G. A. Dunn. 1975. Adhesions of fibroblasts to substratum during contact inhibition observed by interference reflection microscopy. *Exp. Cell Res.* 92:57-62.
49. Rubinstein, N., J. Chi, and H. Holtzer. 1976. Coordinated synthesis and degradation of actin and myosin in a variety of myogenic and non-myogenic cells. *Exp. Cell Res.* 97:387-393.

## CHAPTER 2

### PATTERN AND TIME-COURSE OF RHODAMINE-ACTIN INCORPORATION IN CARDIAC MYOCYTES

## Introduction

Cardiac myocytes isolated from eight-day embryonic chick hearts contain cross-striated myofibrils similar to those found in skeletal muscle (1). Unlike skeletal muscle cells, however, myocytes are capable of DNA synthesis and mitosis after myofibril formation (2). The myocytes retain their myogenic state in culture for up to 6 weeks (3), including their ability to contract spontaneously when sparsely plated, and to contract in coordination with other myocytes when in a high density monolayer (4).

Various studies have investigated the rates of myofibrillar protein synthesis and turnover in embryonic and adult myogenic tissue to elucidate the molecular state of myofibril metabolism. Incorporation of newly synthesized myofibrillar proteins into the contractile apparatus of embryonic cardiac muscle can occur within 2 h after incubation of the cells with a radioactive precursor (5). The major myofibrillar proteins have an identical half-life of 11-12 d in adult heart tissue (6) and of 19 d in skeletal muscle (7), suggesting assembly and degradation of the myofibril as a unit. However, a study of actin and myosin turnover rates in cultured cells showed a half-life for the two proteins of 2.5 to 3 d in replicating, mononucleated cells, and of 6 d in post-mitotic myotubes (8), suggesting that embryonic tissues differ substantially from adult in protein turnover, or that in vitro conditions have stimulated metabolic activity.

The present study was designed to investigate the dynamics of actin incorporation into myofibrils of embryonic cardiac myocytes grown in cell culture. Microinjected rhodamine-actin was rapidly incorporated into

myofibrils of these cells, displaying fluorescent bands that corresponded to the sarcomeres as early as 5 min post-injection. Establishment of the ultimate fluorescent pattern occurred by 10 to 20 min post-injection. Microinjected myocytes, which have incorporated rhodamine-actin into the myofibrils, retained the ability to contract.





Figure 9. General structure of the sarcomere.

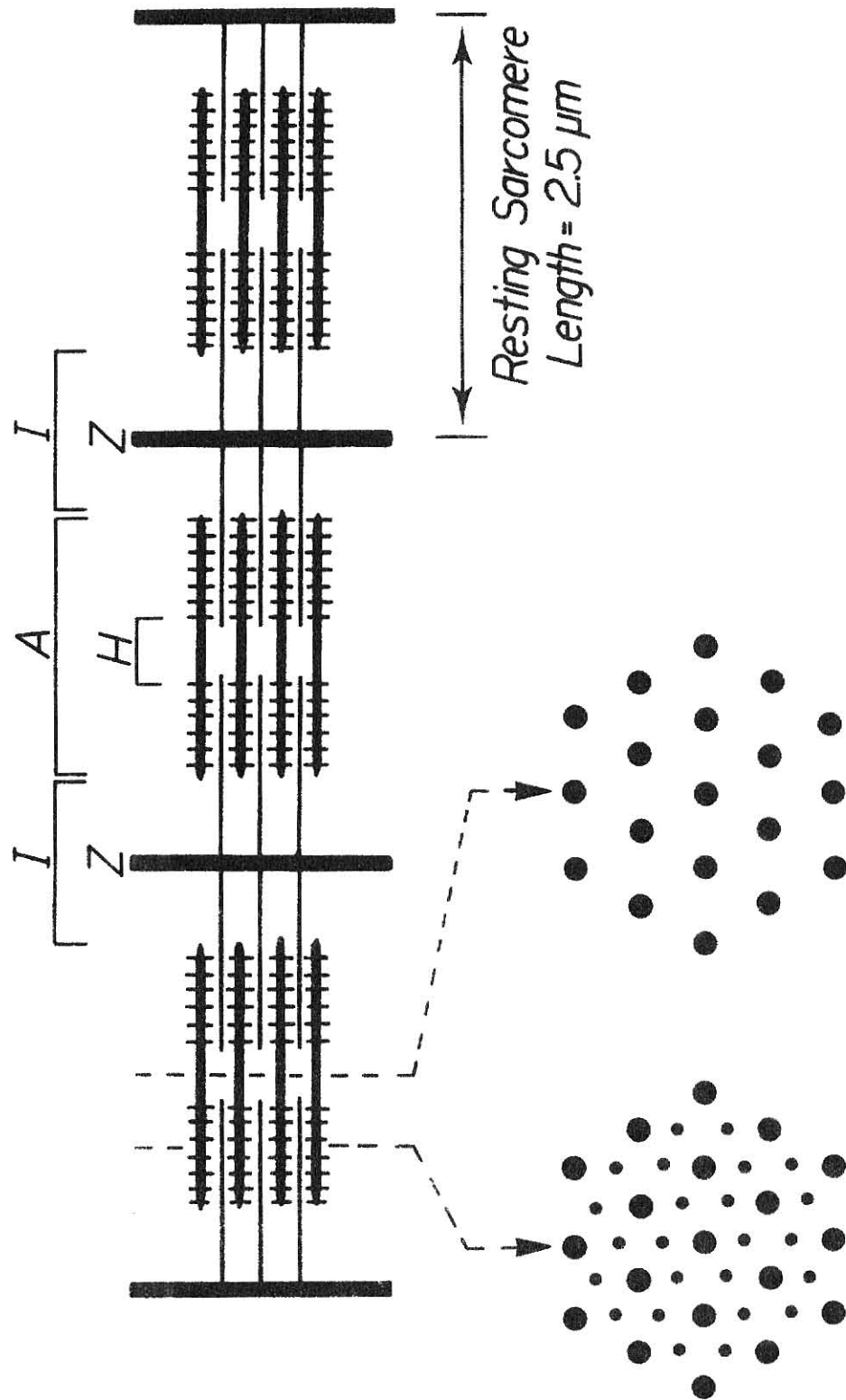
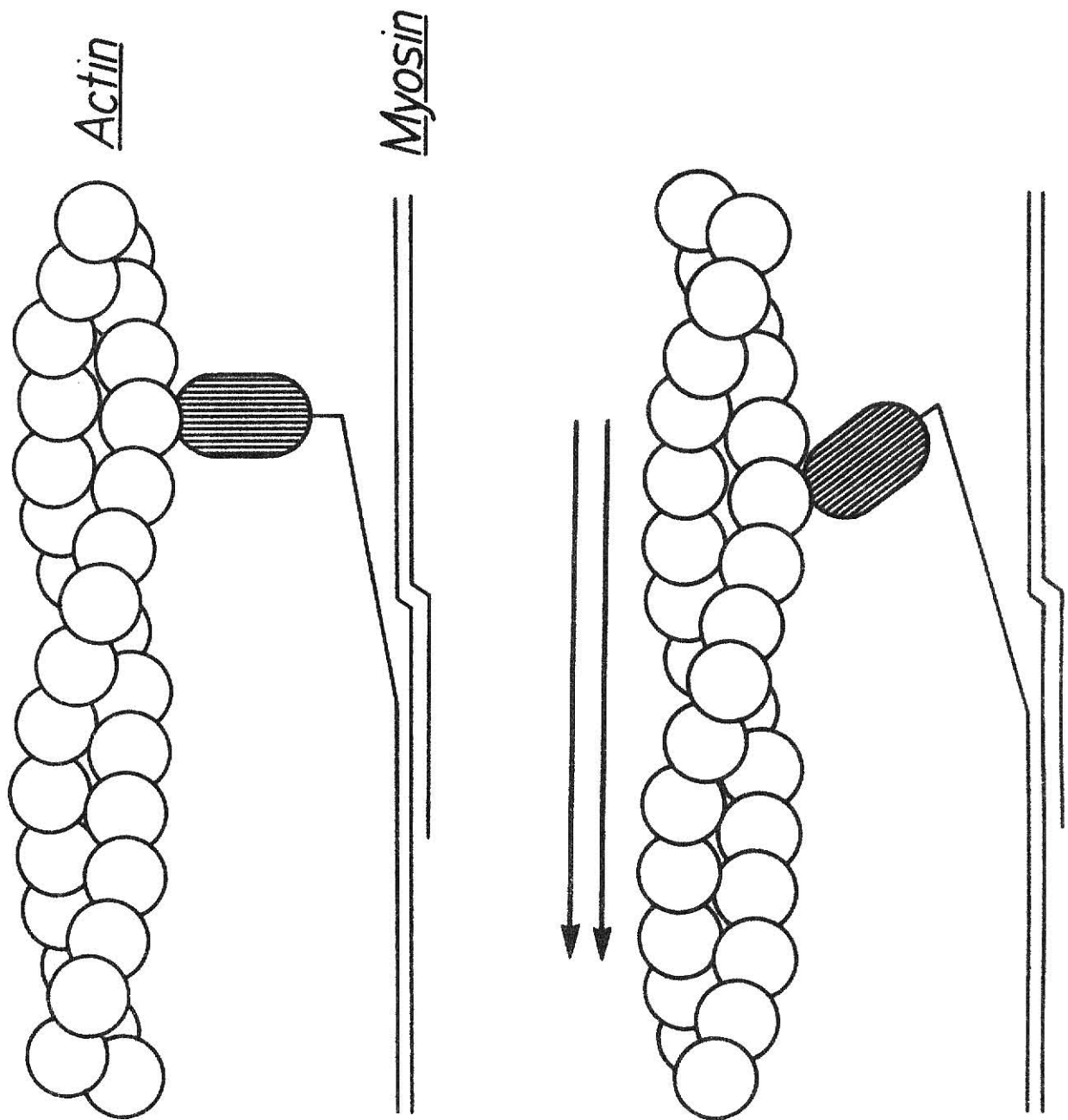




Figure 10. Molecular events leading to sliding of thin and thick filaments. Myosin heads attach to the thin filaments, then a movement at the hinge region of the myosin molecule leads to a translocation of the thin filament.



## Materials and Methods

### Cell Culture Procedures

Hearts from eight-day chick embryos were minced in sterile magnesium- and calcium-free Saline G, and enzymatically dissociated for 15 min at 37° C. Digestions were terminated by addition of an equal volume of F-12 nutrient medium containing 10% fetal calf serum and 30 µg/ml penicillin G and 50 µg/ml streptomycin sulfate. Cell suspensions were filtered through single layers of Nitex cloth, collected by centrifugation, resuspended in fresh nutrient medium and plated onto glass coverslips in 35 mm Falcon tissue culture dishes at a density of  $2-3 \times 10^5$  cells per dish. The dishes were kept in a humid atmosphere of 5% CO<sub>2</sub>/95% air at 37° C. Microinjection was usually performed 24-48 h after plating.

### Fluorescent Labeling of Actin

This procedure has been described . Briefly, approximately 15 mg of skeletal muscle actin (9) was labeled with 10 mg of iodoacetamido tetramethyl rhodamine (Research Organics, Cleveland, Ohio), a sulfhydryl-specific dye which, based upon previous reports of sulfhydryl availability in actin (10,11), should react preferentially with cysteine 373. The rhodamine-actin was purified from free dye, denatured actin and trace contaminants by repeated cycles of polymerization/depolymerization and Sephadex G-25 gel filtration.

### Microinjection and Microscopy

The procedure for microinjection of cardiac myocytes was performed according to standard procedures . A Zeiss Standard microscope, mounted on a Leitz baseplate, was used for microinjection, and both phase and

fluorescence microscopy. Fluorescence exposures were approximately 30-40 seconds using Ilford XP-1 35 mm film developed for 6.5 min at 40° C in Ilford XP-1 chemicals.



## Results

Cardiac myocytes in vitro were assigned two general morphologies: elongated cells with numerous side processes, which frequently made contact with other cells; and myocytes with a fibroblastic morphology, which were difficult to distinguish from non-myogenic cells in the culture. Both types contained numerous cross-striated myofibrils, contracted in a rhythmic and spontaneous fashion, and appeared to incorporate rhodamine-actin identically.

Both beating and quiescent myocytes were microinjected. In the case of beating cells, microinjection either temporarily halted the activity or had no effect. Penetration of the cell membrane of non-beating cells by the micropipette usually was followed by a peristaltic-like wave of contraction that moved down the cell. Glycogen deposits, typically found in cultured myocytes (ref. 3 and Fig.11c), were dispersed when directly in the path of the injected actin solution.

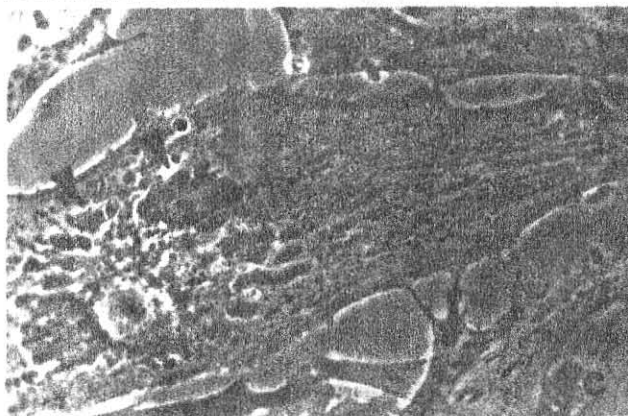
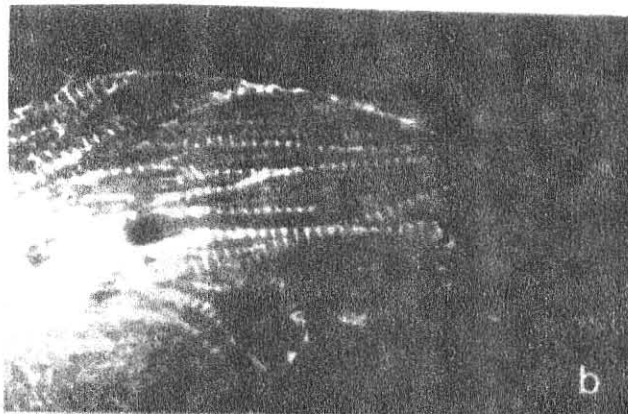
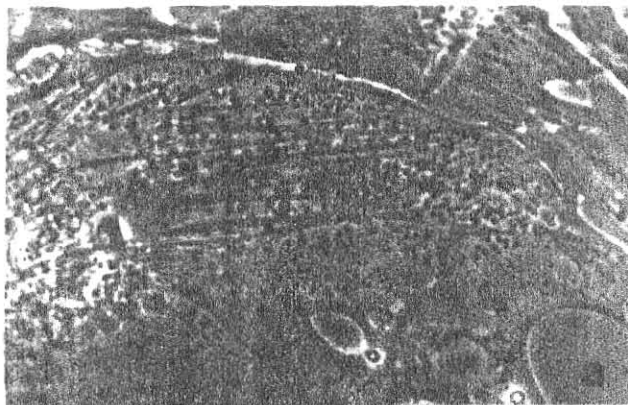
The pattern of rhodamine-actin incorporation into myofibrillar structures immediately following microinjection usually was difficult to discern, due to initial uniform cytoplasmic fluorescence. By 5 min post-injection, however, fluorescent bands periodically distributed along the myofibrils were visible. By 10 min (Fig.11a and b) distinct alternating patterns of fluorescence were seen, particularly in peripheral cell areas containing thinner cytoplasm.

Figures 11c and d represent a myocyte at 1 h post-injection. Exceptionally clear fluorescent patterns are evident in this cell. By comparison to isolated skeletal myofibrils stained with anti-actin antibodies (14), the wide bands of fluorescence in this cell corresponded to actin-containing I-bands. Interestingly, microinjected cells also contained

thin lines of fluorescence which could be seen alternating with the wide bands (Fig. 11d). These narrow bands corresponded to the M-line region in the middle of the H-zone, an area presumably actin-free. At 2 h post-injection (Fig. 11e and f) fluorescent patterns remained essentially unchanged, still demonstrating alternating wide and narrow bands of fluorescence. Observation of injected myocytes up to 15 h post-injection indicated no further qualitative changes in fluorescent distribution. Myocytes at all stages of observation following microinjection retained the ability to contract.



Figure 11. Phase contrast and corresponding fluorescent images of embryonic cardiac myocytes microinjected with rhodamine-actin. Time points following injection are 10 min (a and b), 1 hour (c and d), and 2 hours (e and f). Cells at all three stages show rhodamine-actin incorporation. Narrow bands of fluorescence alternating with wide bands can be seen particularly well in Fig. d. These narrow bands of fluorescence are in a presumably actin-free area, the M-line. Glycogen deposits, typically found in cultured myocytes, are indicated by arrowheads in Fig. c.



### Discussion

This study demonstrates that rhodamine-actin, microinjected into cultured cardiac myocytes, was rapidly incorporated into myofibrils of the cells. Ultimate fluorescence patterns in microinjected myocytes were achieved by 10-20 min post-injection, indicating that a highly dynamic relationship exists between actin of the thin filaments and cellular non-myofibrillar actin. Incorporation of rhodamine-actin into myofibrils had no effect on the ability of microinjected cells to contract.

Myofibrils of cardiac myocytes and skeletal myotubes are morphologically stable structures with very similar ultrastructural features (1). Autoradiographic evidence indicates that following myofibril formation, protein incorporation and metabolic turnover can occur without alteration of myofibril structure (12). It appears that control of myofibrillar protein metabolism is coordinated, from initiation of sarcomeric synthesis (13), to employment of the proteins in and removal from the myofibril (6,7).

Although rhodamine-actin is incorporated rapidly into sarcomeres, the time-course of that incorporation reveals little concerning the detailed steps of the process. If the rhodamine-actin served only as a tracer in endogenous actin pools, and not as a perturbant of cellular functions, then there are at least two possible mechanisms by which rhodamine-actin may integrate into myofibrils. First, actin of the thin filaments may be in a continuous state of exchange with non-myofibrillar actin. This would result in a cycling of cellular actin through sarcomeres, accompanied by little protein degradation. The results of the present study suggest that this exchange is extremely rapid; by 10-20 min post-injection, sarcomeres appear fluorescent to the full width of the I-bands. A second possibility is that incorporation of rhodamine-actin

into the myofibrils is simultaneous with removal and degradative turnover of myofibrillar actin. However, biochemical evidence suggests a half-life for actin of 6 d in cultured myotubes, a period that appears incompatible with the rapid time-course seen in the present study.

Additionally, the likelihood that the time-course of incorporation is artefactual must be considered. Injection of rhodamine-actin may upset the intracellular equilibrium between actin synthesis and utilization by abruptly presenting the cell with an expanded pool of actin. In this case, the cell may very well respond by increasing protein turnover in the myofibril, with concomitant incorporation of the rhodamine-actin from the new pool.

The present microinjection study has demonstrated that myofibrils, heretofore considered static cytoplasmic structures, exhibit a dynamic molecular relationship with non-myofibrillar actin. Presuming actin monomer addition solely at the ends of the thin filaments, the presence of fully fluorescent I-bands by 10-20 min after injection implies that at least some thin filaments are completely turned over once every 10-20 minutes. Our present understanding of this interchange is still rudimentary.

### References

1. Fischman, D. A. 1970. The synthesis and assembly of myofibrils in embryonic muscle. *Curr. Top. Dev. Biol.* 5:235-280.
2. Goode, D. 1975. Mitosis of embryonic heart muscle cells in vitro. An immunofluorescence and ultrastructural study. *Cytobiologie*. 11:203-229.
3. Chacko, S. 1979. Cardiac muscle differentiation and growth in developing chick embryos. In: Muscle Regeneration. Ed., A. Mauro et al. Raven Press, NY. pp. 363-381.
4. Goshima, K. 1975. Further studies on preservation of the beating rhythm of myocardial cells in culture. *Exp. Cell Res.* 92:339-349.
5. Anversa, P., L. Vitali-Mazza, and A. V. Loud. 1975. Morphometric and autoradiographic study of developing ventricular and atrial myocardium in fetal rats. *Lab. Invest.* 33:696-705.
6. Zak, R., E. Ratkizis, and M. Rabinowitz. 1971. Evidence for simultaneous turnover of four cardiac myofibrillar proteins. *Fed. Proc.* 30:1147.
7. Dadoune, J. P. 1980. Protein turnover in muscle cells as visualized by autoradiography. *Intl. Rev. Cytol.* 67:215-257.
8. Rubenstein, N., J. Chi, and H. Holtzer. 1976. Coordinated synthesis and degradation of actin and myosin in a variety of myogenic and non-myogenic cells. *Exp. Cell Res.* 97:387-393.
9. Spudich, J. A., and S. Watt. 1971. The regulation of rabbit skeletal muscle contraction. *J. Biol. Chem.* 246:4866-4871.
10. Wang, Y.-L., and D. L. Taylor. 1980. Preparation and characterization of a new molecular cytochemical probe: 5-iodoacetamidofluorescein-labeled actin. *J. Histochem. Cytochem.* 28:1198-1206.



11. Elzinga, M., and J. H. Collins. 1975. The primary structure of actin from rabbit skeletal muscle. *J. Biol. Chem.* 250:5897-5905.
12. Morkin, E. 1970. Postnatal muscle fiber assembly: Localization of newly synthesized myofibrillar proteins. *Science*. 167:1499-1501.
13. Devlin, R. B., and C. P. Emerson. 1978. Coordinate regulation of contractile protein synthesis during myoblast differentiation. *Cell*. 13:599-611.
14. Spooner, B. S., C. R. Holladay, and G. R. Bright. 1982. Immunofluorescence comparisons of anti-actin specificity. *Eur. J. Cell Biol.* 28:115-121.

APPENDICES

## APPENDIX I

The Microinjection System

## A. Equipment and Preparation

1. Capillary tubes: Omega Dot capillary tubes are used to make the finished micropipettes for microinjection. These capillary tubes contain a fine glass fiber along the inside wall which draws the backloaded injection fluid rapidly to the tip of the pulled micropipette. Generally, thick-walled capillary tubes are avoided because the pulled tip is too fine to allow fluid or even air to pass out the tip. I have obtained the best results using thin-walled capillary tubes (Glass co. of America, Bargaintown, NJ, or F. Haer, Brunswick, ME, 1.2 mm OD x 0.90 mm ID x 10 cm length). The capillary tubes are first soaked in acetone overnight, then in 35 percent nitric acid for four to five hours, after which they are thoroughly rinsed with 3X glass-distilled-water and dried in a small lab oven at 60° C. The capillary tubes are not treated with a siliconizing agent.
2. Micropipettes: Figure A shows the stages in forming a micropipette suitable for microinjection. The capillary tube is first pulled on a DKI Model 700C capillary puller (David Kopf Instruments, Tujunga, CA). The solenoid (or pulling force) is set at zero which allows the capillary tube to be separated into two micropipettes by gravity. The heater setting is 21 amperes which produces a micropipette with a long taper. The micropipette is slightly bent about 1.0-1.5 mm from the tip using a laboratory-built microforge. Then, using a microburner (constructed from a 1-ml plastic syringe) a 30 degree angle is produced in the middle of the micropipette. The resulting micropipette can then be used to microinject cells without fear that the micropipette holder will hit the microscope stage. Figure B shows a side view of the finished micropipette in the injection chamber.
3. Cell Chambers
  - a. Microinjection chamber: This chamber (figure C) is used to support the coverslip containing the tissue culture cells during microinjection and consists of a No. 2 coverglass, 45 mm x 50 mm, upon which is placed a U-shaped plastic support, 2.0 mm thick. The coverslip containing the cells is placed upside-down on the plastic support, then the chamber is filled with a buffered solution such as Saline G. The height of the U-shaped support allows the micropipette to enter the chamber beneath the coverslip.

- b. Viewing chamber: This chamber is similar in construction to the microinjection chamber but has a shallower plastic coverslip support. This support prevents a micropipette from entering the chamber but allows the chamber to be filled with Saline G and the living cells to be viewed under the 63X and 100X oil-immersion objectives (both requiring a short-working-distance condenser).
4. The Microscope: A Zeiss Standard microscope, equipped with epifluorescence illumination, is used for microinjection, viewing and photography. The microscope and a Leitz micromanipulator rest upon a Leitz baseplate. The microscope/baseplate combination in turn sits on a  $\frac{1}{2}$ -inch steel plate which is supported by four 12-inch-diameter air-inflated inner tubes. The microscope table top is cut from a slab of artificial stone and rests upon another set of four inner tubes. Four stacks of cinderblocks serve as legs for the table.
5. Pressure System: The pressure system consists of a plastic 3-ml syringe mounted on a metal tripod support. A micrometer is secured directly behind the syringe with the piston bearing on the syringe plunger. Polyethylene tubing is connected to the front of the syringe via an 18-gauge needle. The other end of the tubing fits through the metal micropipette holder (made from an X-acto blade chuck) which is mounted on the micromanipulator. The shaft of the micropipette fits into the polyethylene tubing and the junction is made tight by screwing down the chuck on the holder. Both the syringe and the polyethylene tubing are filled with Corning 200 fluid.

## B. Microinjection Procedure

The cells to be microinjected are grown on No. 2 coverslips, 22 mm x 22 mm, which have been sterilized in 95 percent ethanol. When using chick fibroblastic cells and myocytes the cells are plated directly onto the coverslips. For muscle cells, the sterilized coverslips are first coated with collagen.

When the cells reach the desired stage for microinjection, the coverslips are removed from the Falcon dishes and placed inverted on the U-shaped support of the microinjection chamber. The chamber is then filled with a buffered solution such as Saline G. The chamber is placed on the microscope stage and the microinjection performed under the 40X dry objective.

Using the micromanipulator, the out-of-focus micropipette is brought into the field of the 40X objective, then slowly raised until it is in the same plane as the cells on the coverslip. With the micropipette in focus, the tip is then positioned beneath the cell to be microinjected and, using the fine verticle control of the micromanipulator, the tip is brought up and into the cell. Hitting the

nucleus of the cell is avoided because the cell easily can be killed if the nucleus is roughly treated.

The micrometer piston is advanced until fluid comes out of the micropipette tip. If the micropipette is firmly in the cell it is possible to see a refractive change spread across the cell. Under UV illumination, a microinjected fluorescent protein can be seen to diffuse slowly across the cell. The amount of time the tip remains in the cell depends on the rate of flow of the sample solution. A slow and steady flow allows the operator sufficient time to gently position the micropipette in the cell, monitor the volume being microinjected and to carefully remove the micropipette.

After microinjection, the coverslip is removed from the microinjection chamber and is placed onto the viewing chamber, which is then placed into a Petri dish with a moist Kimwipe. If I plan to view the cells less than 15 minutes after microinjection, the Saline G is left in the chamber and the entire Petri dish is placed in a 37° C incubator. However, if long-term incubation is planned before viewing and photographing the cells, the Saline G is replaced with nutrient medium and the chamber is placed in a 5% CO<sub>2</sub>/95% air atmosphere at 37° C.

All viewing and photography of the microinjected cells is performed using the 63X or 100X oil-immersion objectives. These objectives increase the level of detectable fluorescence not only because of their high power, but also because the oil is a more efficient medium than air for fluorescent light transmission. If photographs are desired, viewing is kept to a minimum due to the problem of fluorochrome photobleaching.

The solution to be microinjected usually is kept at 4° C in a capped plastic tube. Just prior to microinjection, a small aliquot of the solution is drawn into a glass Pasteur pipet with an extended tip. Then approximately 2-3 µl of the solution is deposited at the 30 degree bend in the micropipette. Within seconds capillary action has drawn the fluid up to the tip and the solution is ready for microinjection. The air left in the shaft of the micropipette does not decrease either the ease of microinjection or the control of volume injected.



Figure A. Stages in micropipette formation.

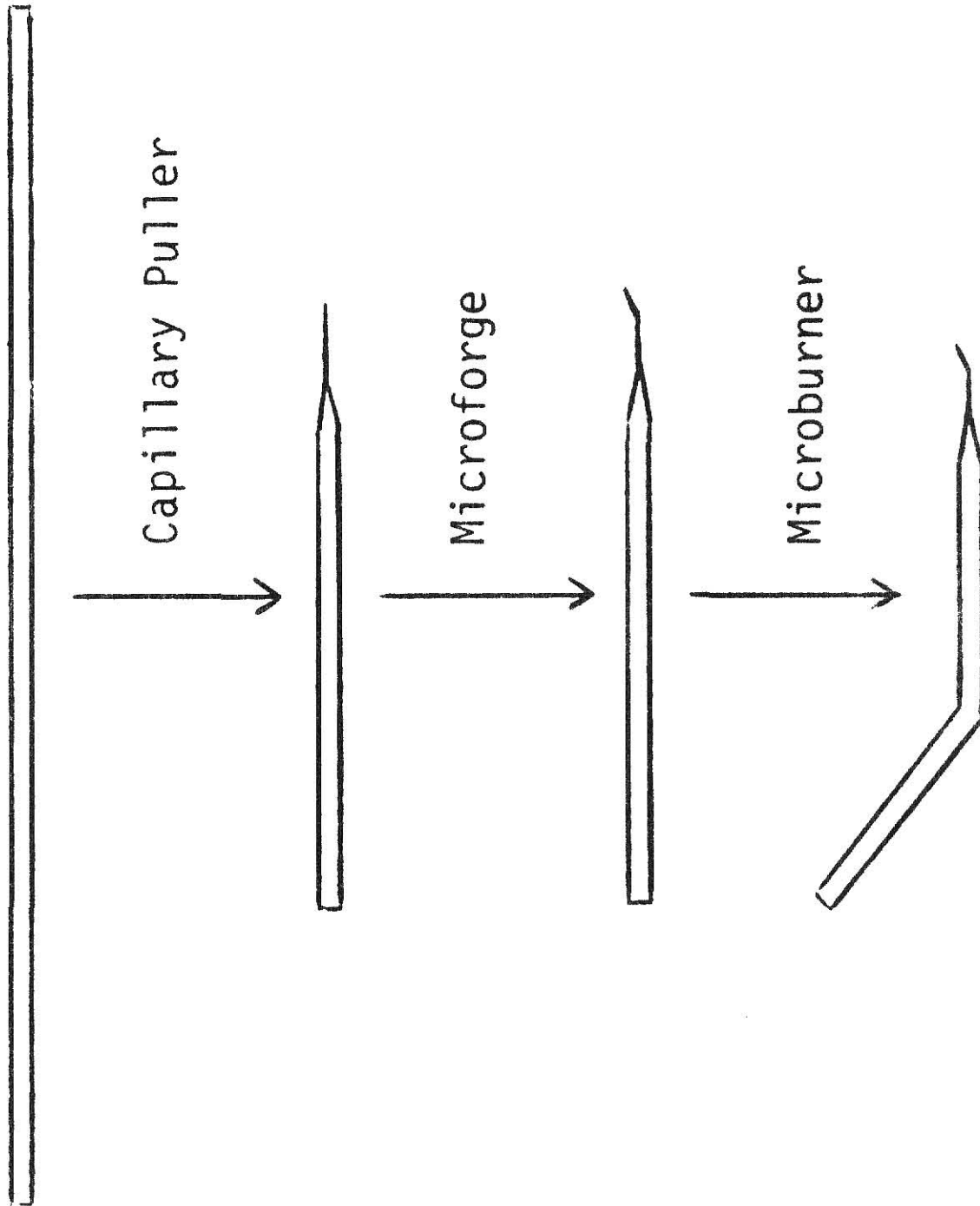


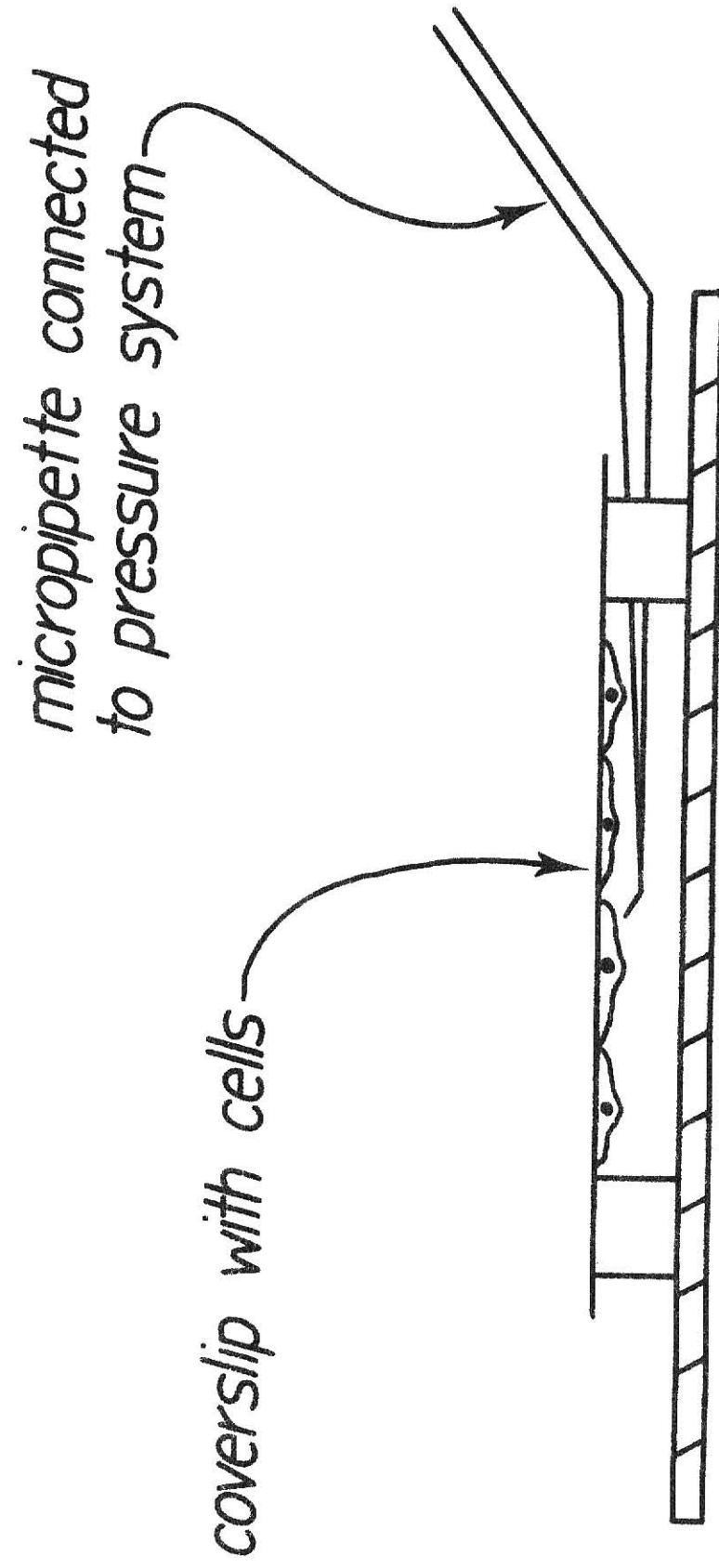


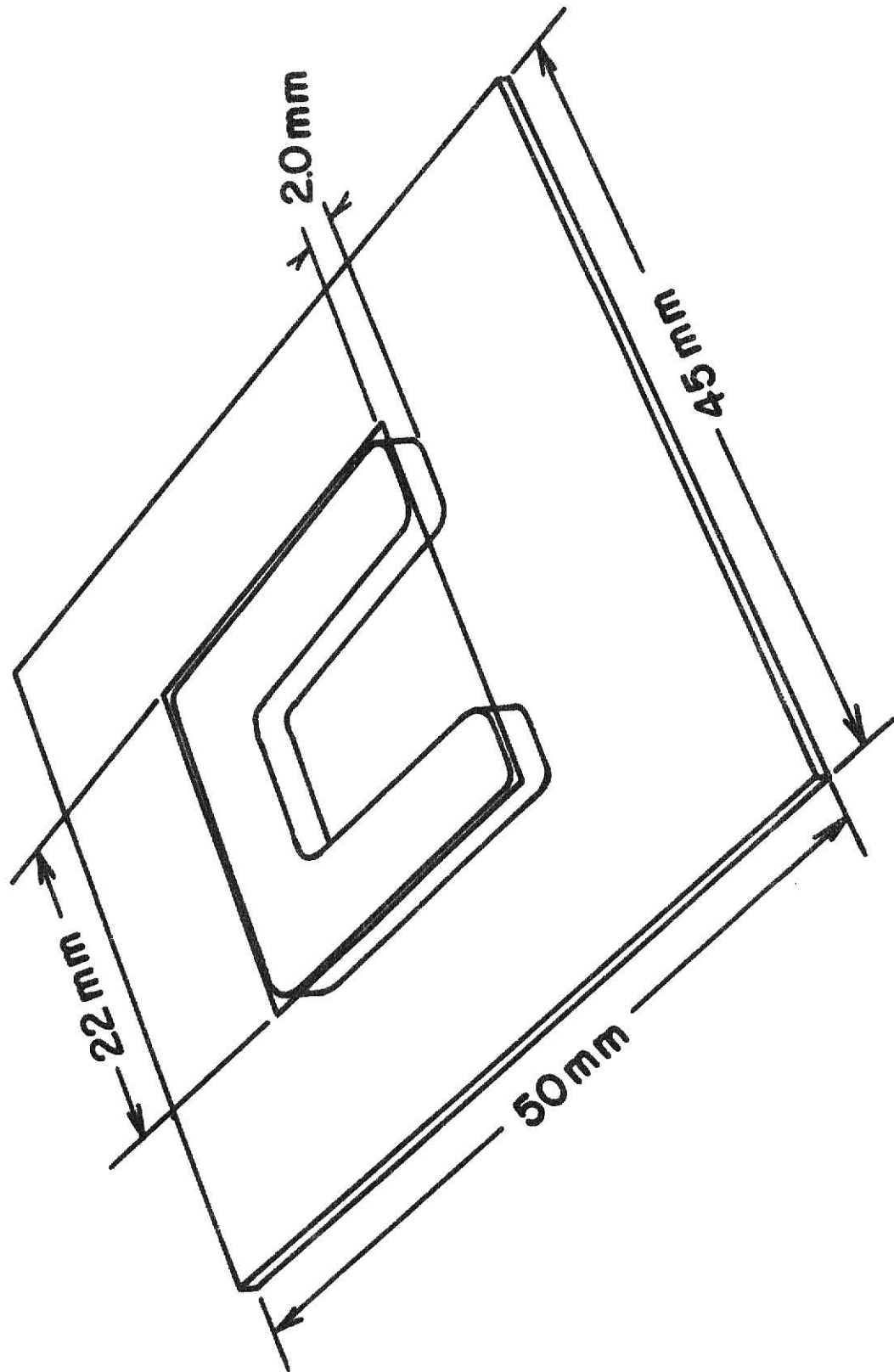


Figure B. Side-view of finished micropipette in microinjection chamber.



Figure C. Microinjection chamber.





## APPENDIX II

Labeling of Actin with Iodoacetamido Tetramethyl Rhodamine

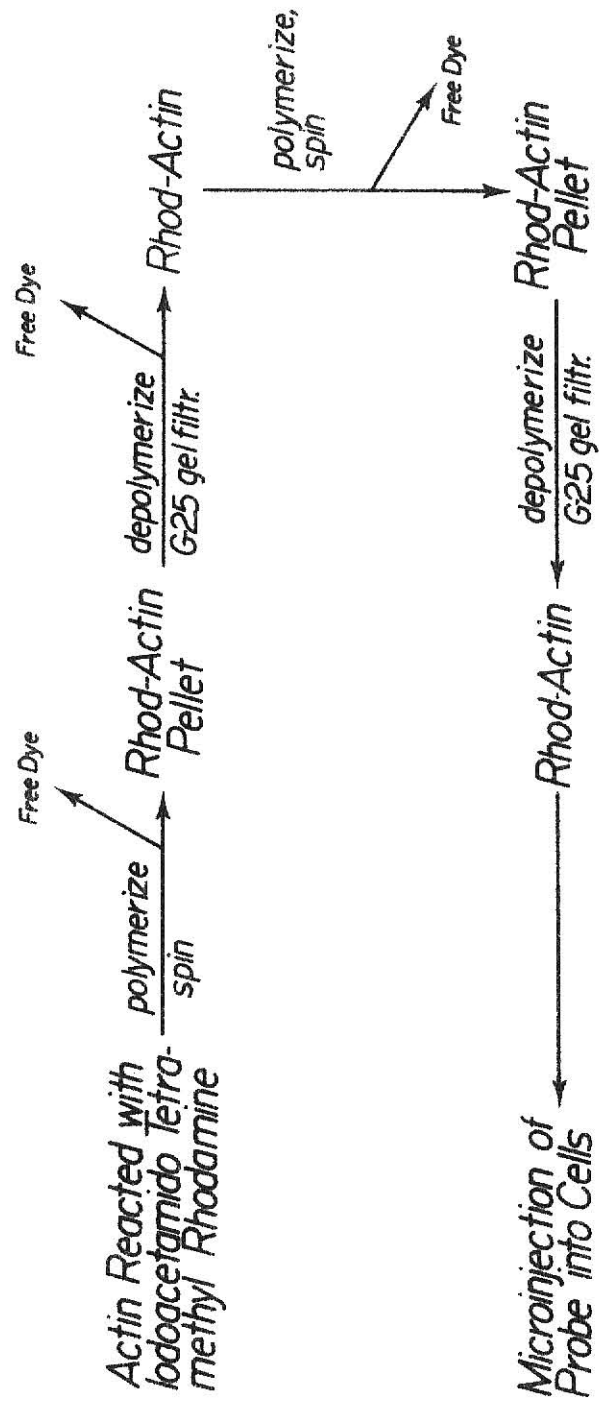
1. Prepare actin in Buffer A (2 mM Tris-base, 0.4 mM Na ascorbate, 0.1 mM  $\text{CaCl}_2$ , 0.2 mM ATP, pH 8.0).
2. Place 10 mg of IAR into 0.5 ml acetone, vortex, then add to 3 ml of Buffer A with 10 mM ATP at pH 10.
3. Add the dye solution dropwise to stirring actin (about 12-15 mg in 6-8 ml), bring the pH to 8.5 and react 2-3 hours at room temperature in the dark.
4. Add 3 M KCl to 100 mM and 1 M  $\text{MgCl}_2$  to 2 mM to the actin solution, stir 5 minutes and let stand for one hour (room temperature).
5. Spin down the rhod-actin at 100,000g for 3 hours at 25° C. Use the SW 27 rotor at 25,000 RPMs in the Beckman ultracentrifuge.
6. Add 2 ml of Buffer A to the pellet, then add slowly with stirring 1 ml of 1.8 M KI, 3 mM  $\text{CaCl}_2$ , 15 mM ATP, pH 7.0. Stir 30 minutes at 4° C.
7. Desalt on a Sephadex G-25 column (1x30 cm) equilibrated with Buffer A (4° C).
8. Clarify the rhod-actin by spinning 100,000g for 2 hours (4° C).
9. Polymerize the rhod-actin by adding 3 M KCl to 100 mM and 1 M  $\text{MgCl}_2$  to 2 mM. Stir 5 minutes, then let stand one hour at room temperature.
10. Spin down rhod-actin by centrifuging 100,000g for 3 hours at 25° C.
11. Depolymerize by adding directly to rhod-actin pellet 0.2-0.3 ml of 0.8 M KI, 10 mM ATP, 1 mM  $\text{CaCl}_2$ , 2 mM 2-ME, pH 7.5 and stir 30 minutes at 4° C.
12. Drop rhod-actin over a 2 ml Sephadex G-25 column equilibrated with 1 mM Tris, 2 mM ATP, 0.1 mM  $\text{CaCl}_2$ , 2 mM 2-ME, pH 7.5. Collect fluorescent fractions.
13. Clarify the rhod-actin by spinning on an airfuge at 80,000g for 30 minutes (4° C).





Figure D. Procedure for labeling actin with IAR.

# LABELING PROCEDURE



## APPENDIX III

Cell Culture Methods

## A. Heart Fibroblastic Cells:

1. Remove heart ventricles from 12-14 day embryonic chicks and mince in sterile calcium- and magnesium-free Saline G.
2. Aspirate CMF Saline G, add 5 ml of 0.2% trypsin in CMF Saline G, and shake cells 30 minutes at 37° C.
3. Halt trypsin activity by adding 5 ml of F12 nutrient medium, filter through a single layer of Nitex cloth in a K-filter and centrifuge 10 minutes at 1500 RPMs in a clinical centrifuge.
4. Resuspend the cell pellet in 5 ml of F12 nutrient medium and determine cell density with a hemacytometer.
5. Plate the cells onto 60 mm Falcon tissue culture dishes (2-4x10<sup>6</sup> cells/dish), place in a humid environment with a 5% CO<sub>2</sub>/95% air atmosphere at 37° C.
6. Allow the cells to grow for 2-4 days.
7. Replate the cells onto No. 2 coverslips in 35 mm Falcon tissue culture dishes (2x10<sup>5</sup> cells/dish).

## B. Cardiac Myocytes:

1. Remove hearts from 7-8 day embryonic chicks and mince in sterile CMF Saline G.
2. Aspirate CMF Saline G, add 5 ml of 0.2% trypsin in CMF Saline G, and shake cells 20 minutes at 37° C.
3. Halt trypsin activity by adding 5 ml of F12 nutrient medium, filter through a single layer of Nitex cloth in a K-filter and centrifuge 10 minutes at 1500 RPMs in a clinical centrifuge.
4. Resuspend the cell pellet in 5 ml of F12 nutrient medium and determine cell density with a hemacytometer.
5. Plate the cells onto No. 2 coverslips in 35 mm Falcon tissue culture dishes (4x10<sup>5</sup> cells/dish).
6. Place the dishes in a humid environment with a 5% CO<sub>2</sub>/95% air atmosphere at 37° C.

## APPENDIX IV

F12 Nutrient Medium

	<u>per liter</u>
GIBCO F12 (Cat. #430-1700)	1 Pkge.
Na bicarbonate	1.176 g
Na ascorbate	0.119 g
Streptomycin sulfate	0.0527 g
Penicillin G	0.0332 g
Fetal calf serum	100 ml
pH 7.2	
Filter sterilize, store frozen.	

## APPENDIX V

Salt Solutions and Buffers

## A. Saline G:

	<u>per liter (g)</u>	
NaCl	8.00	
KCl	0.40	
$\text{Na}_2\text{HPO}_4 \cdot 7\text{H}_2\text{O}$	0.29	(if anhyd. 0.153)
$\text{KH}_2\text{PO}_4$	0.15	
Glucose	1.10	
$\text{MgSO}_4 \cdot 7\text{H}_2\text{O}$	0.154	
$\text{CaCl}_2 \cdot 2\text{H}_2\text{O}$	0.016	(if anhyd. 0.012)
Phenol Red	0.001	
pH 7.2		
Filter sterilize, store cold.		

## B. Phosphate Buffered Saline:

$\text{KH}_2\text{PO}_4 \cdot 3\text{H}_2\text{O}$	0.544	(if anhyd. 0.39)
$\text{NaH}_2\text{PO}_4 \cdot 2\text{H}_2\text{O}$	1.66	
NaCl	7.01	
$\text{NaN}_3$	0.2	
pH 7.25		

## C. Buffer A

	<u>concentrations (mM)</u>
Tris-base	2.0
Na ascorbate	0.4
$\text{CaCl}_2$	0.1
ATP	0.2
pH 8.0	

## D. Buffer G

Tris-base	2.0
2-Mercaptoethanol	0.2
$\text{CaCl}_2$	0.1
ATP	0.2
pH 8.0	

## APPENDIX VI

Trypsin Solutions

## A. Dissociation of embryonic tissue:

0.2% trypsin in CMF Saline G.

pH 7.2

Filter sterilize, store frozen in 5 ml aliquots.

## B. Transfer of cells:

0.2% trypsin/0.2% EDTA in CMF Saline G.

pH 7.2

Filter sterilize, store frozen.

## APPENDIX VII

Skeletal Muscle Acetone Powder

1. Remove breast muscle from adult chickens or dorsal muscle from rabbits, cut into chunks and mince twice through a meat grinder (4° C).
2. Suspend the mince in three volumes of 0.1 M KCl, 0.15 M potassium phosphate, pH 6.5, and stir 10 minutes (4° C). Filter the suspension through two layers of cheesecloth which have been boiled for 20 minutes and cooled to 4° C.
3. Extract the mince with six volumes of 0.05 M NaHCO<sub>3</sub> by stirring 10 minutes and filtering as above (4° C).
4. Extract the mince with three volumes of 1 mM EDTA, pH 7.0 by stirring 10 minutes and filtering as above (4° C).
5. Extract the mince twice with six volumes of distilled water, stirring 5 minutes each time (4° C).
6. Extract the mince five times with three volumes of acetone, stirring 10 minutes for each extraction. The acetone should be cold but the procedure can be carried out at room temperature.
7. Dry the filtered residue on a piece of aluminum foil overnight in a hood, then store desiccated at -20° C.

Note: Adjust pH of all solutions at room temperature.

## APPENDIX VIII

Skeletal Actin Isolation from Acetone Powder

1. Mix 10 g of acetone powder with 200 ml of Buffer G (2 mM Tris, 0.2 mM ATP, 0.2 mM 2-ME, 0.1 mM  $\text{CaCl}_2$ , pH 8.0) and stir 1 hour at 4° C.
2. Spin down the muscle residue at 10,000 RPMs for 30 minutes in the SS-34 rotor (4° C) and save the supernate.
3. Re-extract the residue with 100 ml of Buffer G and repeat step 2.
4. Combine the supernates from steps 2 and 3 and filter through a Whatman No. 1 filter. Discard muscle.
5. Concentrate the supernates to about 50 ml on an Amicon cell (4° C).
6. Polymerize the actin by adding with stirring 3 M KCl to 0.6 M and 1 M  $\text{MgCl}_2$  to 2 mM. Let stand at room temperature for two hours.
7. Centrifuge the actin at 100,000 g for 3 hours at room temperature. Use the SW 27 rotor for 3 hours at 25,000 RPMs in a Beckman ultracentrifuge.
8. Resuspend the pellet in Buffer G with homogenization (4° C).
9. Dialyze against Buffer G (2x4 l) for 48-72 hours (4° C).
10. Clarify the actin by spinning 1 hour at 15,000 RPMs in the Sorvall SS-34 rotor (4° C).
11. At this point the actin can be further purified by repeated polymerization/depolymerization or by Sephacryl S-200 gel filtration.



## APPENDIX IX

Bio-Rad Protein Assay

1. Prepare dilute, filtered dye. Mix one volume of dye concentrate with four volumes of glass-distilled-water and filter through a Whatman No. 1 (make about 80 ml total).
2. Prepare BSA standard in the buffer of the experimental protein at a concentration of 2 mg/ml. Set up the following series:

<u>Series</u>	<u>Protein Conc.</u>	<u>BSA Stock</u>	<u>Buffer</u>
Blank	0 $\mu\text{g/ml}$	0.0 ml	5.0 ml
1	200	0.5	4.5
2	400	1.0	4.0
3	600	1.5	3.5
4	800	2.0	3.0
5	1000	2.5	2.5
6	1200	3.0	2.0

One tube for each series.

3. Place 50  $\mu\text{l}$  of protein standards into a test tube, then add 2.5 ml of the diluted dye. Use three tubes for each protein concentration.
4. Vortex lightly and read at 595 nm after 10 minutes.
5. Repeat steps 3 and 4 for the experimental protein.

## APPENDIX X

Viscometry Assay of Actin

1. Dialyze actin against Buffer A or Buffer G to completely depolymerize, then spin 20,000 RPMs for one hour in the SS-34 rotor (4° C) to remove insoluble material.
2. Prepare 2 ml samples of G-actin at known concentrations in the range 0.1-0.5 mg/ml. Polymerize the actin by adding 3 M KCl to 100 mM and 1 M MgCl<sub>2</sub> to 2 mM. Use 70 µl of 3 M KCl and 4 µl of 1 M MgCl<sub>2</sub>. After salt addition multiply initial actin concentration by 0.965 to get the final actin concentration.
3. Incubate the samples 4-8 hours at 25° C.
4. Prepare viscometer and buffer at 25° C by using a running water bath.
5. Measure viscometry of buffer, then of samples. Charge the viscometer twice for each protein concentration and measure the viscosity of each charge twice.
6. Clean the viscometer between each charge by rinsing with water, then acetone and drying with a stream of nitrogen.
7. Calculate specific viscosity:

$$\eta_{sp} = \frac{\eta_{sample} - \eta_{solvent}}{\eta_{solvent}}$$

$\eta_{sp}$  = specific viscosity

$\eta_{sample}$  = flow time for actin solutions

$\eta_{solvent}$  = flow time for buffer

## APPENDIX XI

Incubation of Fixed, Permeabilized Cells with Rhod-Actin

1. Grow cells on No. 2 coverslips.
2. Rinse twice in PBS (0.15 M NaCl, 0.01 M Na Phosphate)(37° C).
3. Immerse coverslips in 0.5% Triton X-100, 0.37% formaldehyde in PBS for five minutes (37° C).
4. Post-fix in 3.7% formaldehyde in PBS for 20 minutes (37° C).
5. Rinse twice in PBS (37° C).
6. Rinse thrice in Buffer G (37° C).
7. Incubate cells with rhod-actin in Buffer G for ten minutes (37° C).
8. Rinse cells thrice with Buffer G (37° C).
9. Mount coverslips with 50% glycerol/50% PBS and view on microscope.

DISTRIBUTION OF FLUORESCENTLY LABELED ACTIN  
IN LIVING CELLS

by

STEPHEN DOUGLAS GLACY

B.S., Kansas State University, 1979

AN ABSTRACT OF A MASTER'S THESIS  
submitted in partial fulfillment of the  
requirements for the degree  
MASTER OF SCIENCE

Division of Biology  
KANSAS STATE UNIVERSITY  
Manhattan, Kansas

1982

### Abstract

The time-course and pattern of incorporation of rhodamine-labeled actin microinjected into cultured fibroblastic cells and cardiac myocytes were examined by fluorescence microscopy. Following microinjection of rhodamine-actin into fibroblastic cells, the fluorescent probe was incorporated rapidly into ruffling membranes, and within five minutes, faintly fluorescent stress fibers were observed. Levels of fluorescence in ruffling membranes then tended to remain constant while fluorescence of the stress fibers continued to increase until about 20 min post-injection. Small, discrete regions of some microinjected fibroblastic cells displayed high levels of fluorescence that initially appeared about 5-10 min post-injection. These small areas of intense fluorescence frequently were observed near the cell periphery and corresponded to focal contacts when visualized with interference reflection optics. The results from this portion of the microinjection study show that a relationship exists between patterns of fluorescent actin incorporation in these cells and cellular areas or structures presumed to play a role in cell movement. These findings suggest that actin within stress fibers and the microfilament network of ruffling membranes undergoes a rapid turnover that may relate directly to the motility of the cells.

Microinjection of skeletal actin labeled with rhodamine into cultured cardiac myocytes was followed by rapid incorporation of fluorescence into myofibrils of the cells. Myocytes examined as soon as five min post-injection displayed fluorescent bands corresponding to the sarcomeres. By 10 min, distinct alternating wide and narrow bands of fluorescence were observed. The wide bands appeared to correspond to the full breadth of the I-bands, whereas the narrow bands of fluorescence corresponded to the M-line. This pattern of fluorescence remained essentially unchanged for

at least 15 h post-injection. The myofibrils of cardiac myocytes were functional after rhodamine-actin incorporation as judged by their ability to contract. The results of this part of the microinjection study suggest that cardiac myofibrils are morphologically stable structures which, nonetheless, exhibit a dynamic equilibrium with non-polymerized cellular actin.